

# A Microscopic Theory of the Neutron

**J.X. Zheng-Johansson**

Institute of Fundamental Physics Research, 611 93 Nyköping, Sweden

## **Abstract.**

A microscopic theory of the neutron, which consists in a neutron model constructed using key relevant experimental observations as input information and in terms of the model neutron the first principles solutions for the basic properties, is proposed within a framework consistent with the Standard Model. The neutron is composed of an electron  $e$  and a proton  $p$  that are separated at a distance  $r_1$  of the order  $10^{-18}$  m, and are in relative orbital angular motion and Thomas precession highly relativistically, with their reduced mass moving along a quantised  $l = 1, j = \frac{1}{2}$  circular orbit of radius  $r_1$  about their centre of mass. The associated rotational energy flux, or vortex, has a spin  $\frac{1}{2}$  and is identifiable as a confined antineutrino. The particles  $e, p$  are attracted with one another predominantly by a central magnetic force produced as result of the particles' relative orbital, precessional and intrinsic angular motions. The interaction force (resembling the weak force), potential (resembling the Higgs' field), and a corresponding excitation Hamiltonian ( $H_I$ ), among others, are derived based directly on first principles laws of electromagnetism, quantum mechanics and relativistic mechanics within a unified framework. In particular, the equation for  $\frac{4}{3}\pi r_1^3 H_I$ , which is directly comparable with the Fermi constant  $G_F$ , is predicted as  $G_F = \frac{4}{3}\pi r_1^3 H_I = A_o C_{0\frac{1}{2}}/\gamma_e \gamma_p$ , where  $A_o = e^2 \hbar^2 / 12\pi \epsilon_0 m_e^0 m_p^0 c^2$ ,  $m_e^0, m_p^0$  are the  $e, p$  rest masses,  $C_{0\frac{1}{2}}$  is a geo-magnetic factor, and  $\gamma_e, \gamma_p$  are the Lorentz factors. Quantitative solution for a stationary meta-stable neutron is found to exist at the extremal point  $r_{1m} = 2.537 \times 10^{-18}$  m, at which the  $G_F$  is a minimum (whence the neutron lifetime is a maximum) and is equal to the experimental value. Solutions for the magnetic moment, effective spin ( $\frac{1}{2}$ ), fine structure constant, and intermediate vector boson masses of the neutron are also given in this paper.

## **1. Introduction**

The neutron ( $n$ ) is a building particle of matter, as the proton ( $p$ ) and electron ( $e$ ) are. The neutron  $n$  yet distinguishes from the  $p, e$  prominently in its undergoing weak decay, under which parity notably is not conserved. In inverse proportion to the weak interaction strength represented by the Fermi constant  $G_F$ , the lifetime of a free neutron is of a finite 12 minutes only. The Fermi constant  $G_F$  combined with the Heisenberg relation indicates moreover a weak interaction distance of an order  $10^{-18}m$ . Weak decay is in fact a underlining property of all of the other several hundred elementary matter particles observed in the laboratory except for the proton and electron, by virtue of which process these systems are unstable, short lived. The basic properties of the weak processes, foremost the neutron  $\beta$  decay, have been experimentally studied extensively over the past eight decades or so, and summarised under the Standard Model (SM) for elementary particles [1]. Theoretically, the weak decay of neutron and other particles has been accounted satisfactorily for, most notably in quantitative prediction of the branching ratio, by the unified renormalisable theories of weak interaction. The Glashow-Weinberg-Salam (GWS) electroweak theory [2a-c] based on group  $SU(2) \times U(1)$  is one of these. This theory in particular also predicts the charged and neutral intermediate vector bosons  $W^-, W^+$  and  $Z^0$

which were confirmed by the experiments at CERN; its renormalisability was proven by t'Hooft in 1971 [2d]. All of the current field theories of the neutron are essentially focused with the neutron  $\beta$  decay, and are rested on the original hypothesis of Fermi[2e]. Namely that, in a neutron  $\beta$  decay reaction  $n \rightarrow p + e + \bar{\nu}_e$ , the matter particles  $e, p$  and the antineutrino  $\bar{\nu}_e$  do not exist until the neutron  $n$  decays. And upon neutron decay, these particles are envisaged as simply emitted by the neutron (as a point entity) in an analogous way to an accelerated point charge emitting electromagnetic radiation. The current theory of the neutron remains as a phenomenological one. There remain certain outstanding questions yet to be resolved. In particular, the origin of the weak interaction force is not well understood, the equation of the weak force accordingly is yet to be derived, and the Fermi constant  $G_F$  is yet to be derived based on the interaction force. At a similar significant level, the nature and the origins of the (anti)neutrino, the intermediate vector bosons, the Weinberg weak mixing angle, and the Higgs mass are not yet fully well understood. One common feature suggestive of the nature of the weak phenomena however is readily recognisable directly from observations, namely that the weak phenomena present only with the electrons and protons in the baryon ( $n, \Lambda$ , etc) and meson ( $\pi, K$ , etc.) disintegration processes, but not with the same electrons and protons in free-particle or bound atomic processes. For a more comprehensive understanding of the nature of the weak phenomena, a microscopic theory would be indispensable. The purpose of this paper is to develop a microscopic theory of the neutron, serving as a prototype of the weak process participating systems, based firstly on a realistic real-space model construction of the neutron, such that the fundamental weak force and the variety of weak-interaction related properties and phenomena can be predicted based on first principles solutions within a unified framework of electromagnetism, quantum mechanics, and relativistic mechanics.

Using several key relevant experimental facts, in particular the neutron beta decay reaction equation  $n \rightarrow p + e + \bar{\nu}_e$ , the neutron spin ( $\frac{1}{2}$ ), the order of magnitude of the Fermi constant  $G_F$  and the so implied weak interaction distance  $\sim 1 \cdot 10^{-18}$  m as direct input information, we propose at the outset of the theory development a real-space ( $e, p$ -) neutron model as follows: The *neutron* is composed of an electron  $e$  and a proton  $p$  separated at a distance  $r(= r_1)$  of the order  $10^{-18}$  m; see Fig 1a. The  $e, p$  are in relative orbital angular motion and in addition a Thomas precession at a velocity approaching the velocity of light  $c$ , under a central force of an electromagnetic origin. The central force is in effect predominantly an attractive magnetic force produced by the magnetic fields ( $\mathbf{B}_p, \mathbf{B}_e$ ) of  $p, e$  at  $e, p$  as result of their intrinsic spin and relative motions. The  $z$ -components ( $S_{ez}, S_{pz}$ ) of the  $e, p$  spin angular momenta are aligned parallel to each other and antiparallel to that of their relative motion ( $J_{z-\frac{1}{2}}$ , Figs 1b), so that the magnetic interaction force is maximally attractive. The  $e, p$  relative motion is in such a way that their reduced mass ( $\mathcal{M}$ ) moves at a velocity ( $\mathbf{v}_{\frac{1}{2}}$ ) accordingly approaching  $c$  along a (quantised  $l = 1, j = \frac{1}{2}$ ) circular orbit of radius  $r(= r_1)$  about their (the  $e, p$ ) common centre of mass (CM), with a normal ( $\mathbf{n}$ ) at a precession-modified quantised angle ( $\pi - \theta_{\frac{1}{2}}$  for  $j$  spin down state) to the  $z$  axis; see Fig 1b. The relative precessional-orbital angular momentum projected in  $z$  direction ( $J_{z-\frac{1}{2}}$ ) will show to be a negative half-integer quantum  $J_{z-\frac{1}{2}} = -\frac{1}{2}\hbar$ . The corresponding neutral rotational energy flux, or vortex, along the  $l = 1, j = \frac{1}{2}$  circular orbit, of accordingly a  $z$ -component angular momentum  $J_{z-\frac{1}{2}}$ , resembles a "confined antineutrino" ( $\bar{\nu}_e$ ).

It is commented that, the proposed  $e, p$ -neutron model suggests also a scheme for the strong force similarly on a unified basis with electromagnetism: A proton  $p$  would be attracted with a neutron  $n(e, p)$  (mainly) through an electrostatic attraction with the electron  $e$  of the neutron at short range; in the same order of the short-range electrostatic interaction, two protons will repel, but never attract with one another. Such characteristics are in accordance with the observational fact that no nucleus exists which is made of more than one protons and protons only without neutrons. The author's more recent research (internal work) has further shown that a microscopic representation of the muon and the "muon-emitting" (composite) elementary

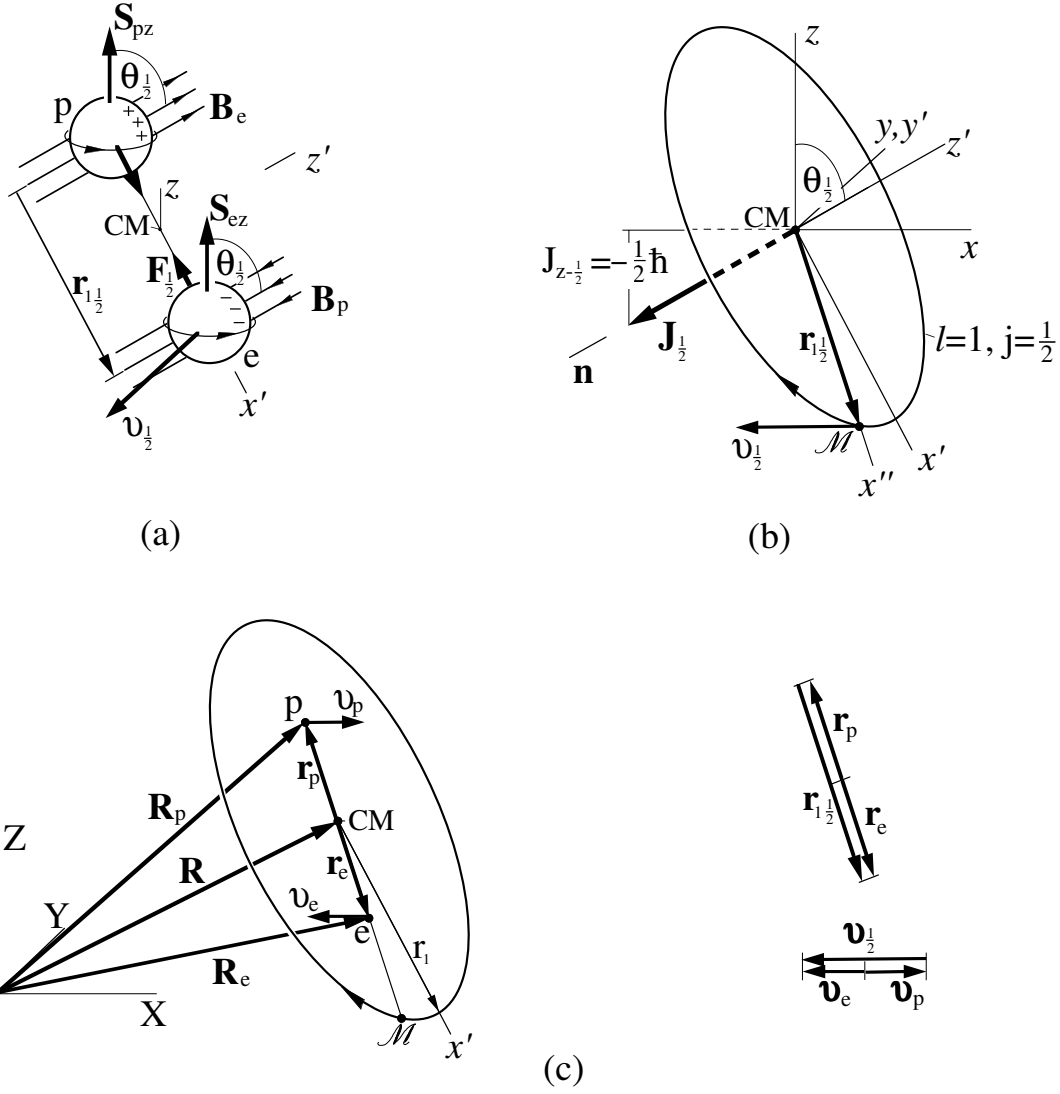


**Figure 1.** Schematic of the model neutron composed of an electron  $e$  and a proton  $p$ . (a) The  $e, p$  are separated by a distance  $r_{1\frac{1}{2}} = r_1 \hat{r}_{1\frac{1}{2}}$  (drawn along  $x'$  direction) and are in relative angular motion and a Thomas precession at velocity  $\mathbf{v}_{1\frac{1}{2}}$  under a magnetic interaction force  $\mathbf{F}_{1\frac{1}{2}}$  in the magnetic fields  $\mathbf{B}_p, \mathbf{B}_e$  of  $p, e$  on  $e, p$ ; their spins  $\mathbf{S}_{ez}, \mathbf{S}_{ps}$  (in units  $\hbar$ ) are aligned parallel in the  $+z$  direction as shown, and antiparallel to  $J_{z-\frac{1}{2}}$  of graph (b). (b) The reduced mass  $\mathcal{M}$  of  $e, p$  moves at velocity  $\mathbf{v}_{1\frac{1}{2}}$  about the  $CM$  along a  $l = 1, j = \frac{1}{2}$  circular orbit of radius vector  $\mathbf{r}_{1\frac{1}{2}}$  and normal  $\mathbf{n}$  at angle  $\pi - \theta_{1\frac{1}{2}}$  to the  $z$  axis; it has a  $z$ -component angular momentum  $J_{z-\frac{1}{2}}$ . (c) Left: The  $e, p$  are located at positions  $\mathbf{r}_e, \mathbf{r}_p$ , moving at velocities  $\mathbf{v}_e, \mathbf{v}_p$ , relative to the  $CM$  in the  $CM$  frame (coordinates  $x, y, z$  in graph b), and at  $\mathbf{R}_e, \mathbf{R}_p$  in the lab frame (coordinates  $X, Y, Z$ ). Right: vector relations between  $\mathbf{r}_e, \mathbf{r}_p$  and  $\mathbf{r}_{1\frac{1}{2}}$ , and  $\mathbf{v}_e, \mathbf{v}_p$  and  $\mathbf{v}_{1\frac{1}{2}}$ . The drawings are made for  $m_e \simeq m_p$ .

particles may be achieved within a consistent scheme with the neutron model. The system of the so-represented elementary particles furthermore is in conformity with the quark model, in a manner that the (internal) spin states of the (composite) elementary particles are in one-to-one correspondences with the configurations of the (observationally-never-isolatable) quarks. The internal spin states of the model neutron under reversed signs (which represents the neutron

effective spin, see Sec 3),  $-\frac{1}{2}, -\frac{1}{2}, \frac{1}{2}$  (i.e. "down, down, up"), for example, directly correspond with the  $ddu$  quarks. The (free) proton, as another example, is a non-composite particle with only one spin state, assigned as  $+\frac{1}{2}$  (spin up) by convention. But this may be translated into a systematic three-spin states representation as  $\frac{1}{2}, \frac{1}{2}, -\frac{1}{2}$  (i.e. "up, up, down"), by adding two dummy spins  $\frac{1}{2}, -\frac{1}{2}$  without changing the original spin  $\frac{1}{2}$ ; the three spin states correspond directly to the  $uud$  quarks.

The remainder of this paper gives a first-principles mathematical representation of the model neutron, mainly in respect to the internal relativistic kinematics, dynamics (Secs 2), magnetic structure (Sec 3), and a derivation of the internal  $e, p$  interaction force (Sec 4) of the neutron in stationary state, the dynamics upon the neutron  $\beta$  decay (Secs 5), and a quantitative evaluation of the dynamical variables (Sec 6). The (quantitative) predictions of the basic properties of the neutron are subsequently subjected to comparisons with, or constraints by, the available experimental data where in question, so that critical checks and controls of the viability of the neutron model are made as far as possible. Other basic aspects, including the parity associated with the  $\beta$  decay, a direct derivation of the intermediate vector boson masses and Weinberg mixing angle of the neutron, and a corresponding dynamic scheme for the other (composite) elementary particles participating weak interaction, will be elucidated in separate papers.

## 2. Equations of motion. Coordinate transformations. Solutions

*2.1. Transformed Newtonian equations of motion of the mean and instantaneous positions*  
 Consider that an electron  $e$  and a proton  $p$  comprising a neutron are at time  $t$  located with the probability densities  $|\psi_\alpha(\mathbf{R}_\alpha, t)|^2$  ( $\alpha = e, p$ ) at positions  $\mathbf{R}_e, \mathbf{R}_p$  relative to the coordinates  $X, Y, Z$  fixed in the laboratory (lab) frame; see Fig 1c. (The usual statistical point-particle picture suffices and is referred to here.) The  $e, p$  are in relative motion at a velocity to prove high compared to  $c$  (Sec 6) under a mutual interaction force  $\mathbf{F}$  and gravity  $\mathbf{g}$ ; no applied force presents. Their mean positions,  $\bar{\mathbf{R}}_\alpha = \int \mathbf{R}_\alpha |\psi_\alpha|^2 d^3 R_\alpha$ , evolve according to the transformed Newtonian equations of motion,  $\frac{d(m_\alpha(d\bar{\mathbf{R}}_\alpha/dt))}{dt} = \int (m_\alpha \mathbf{g} \pm \mathbf{F}) |\psi_\alpha|^2 d^3 R_\alpha$  (the correspondence principle), where  $m_e, m_p$  are the  $e, p$  masses. The  $e, p$  are assumed to form a bound stationary system until Sec 5 and hence feasibly move circularly at constant (tangential) velocities ( $\mathbf{u}_\alpha = d\mathbf{R}_\alpha/dt$ ). The equations of motion thus reduce to

$$m_e \frac{d^2 \mathbf{R}_e}{dt^2} = m_e \mathbf{g} + \mathbf{F}, \quad m_p \frac{d^2 \mathbf{R}_p}{dt^2} = m_p \mathbf{g} - \mathbf{F}. \quad \text{Or} \quad M \frac{d^2 \mathbf{R}}{dt^2} = M \mathbf{g}, \quad \mathcal{M} \frac{d^2 \mathbf{r}}{dt^2} = \mathbf{F}, \quad (1)$$

where

$$\mathbf{R} = \frac{m_e \mathbf{R}_e + m_p \mathbf{R}_p}{M}, \quad M = m_e + m_p, \quad \mathbf{r} = \mathbf{R}_e - \mathbf{R}_p = \mathbf{r}_e - \mathbf{r}_p, \quad \mathcal{M} = \frac{1}{m_e} + \frac{1}{m_p} = \frac{m_e m_p}{M};$$

$$\mathbf{R}_e = \mathbf{R} + \frac{m_p}{M} \mathbf{r}, \quad \mathbf{R}_p = \mathbf{R} - \frac{m_e}{M} \mathbf{r}; \quad \mathbf{r}_e = \mathbf{R}_e - \mathbf{R} = \frac{m_p}{M} \mathbf{r}, \quad \mathbf{r}_p = \mathbf{R}_p - \mathbf{R} = -\frac{m_e}{M} \mathbf{r}. \quad (2)$$

$\mathbf{R}$  is the position of the centre of mass, CM;  $M$  is the total mass located at  $\mathbf{R}$ ;  $\mathbf{r}$  is the relative position;  $\mathcal{M}$  is the reduced mass (of a fictitious particle) located at  $\mathbf{r}$ ; and  $\mathbf{r}_e, \mathbf{r}_p$  are the  $e, p$  positions relative to  $\mathbf{R}$ . Eqs (1c,d) are given for the masses  $M$  and  $\mathcal{M}$  travelling accordingly circularly or along closed path at constant velocities ( $\mathbf{u}_M = d\mathbf{R}/dt$  relative to the lab frame and  $\mathbf{v}$  about the CM). A common time  $t$  measured by a clock fixed at the CM has been used in order to facilitate the direct transformation of Eqs (1a,b) to (1c,d). Accordingly, this specific time  $t$  enters as the independent variable of  $\mathbf{g}, \mathbf{F}$  in Eqs (1a,b):  $\mathbf{g} = \mathbf{g}(t), \mathbf{F} = \mathbf{F}(t)$ ; the local times ( $t_e, t_p$ ) at  $\mathbf{r}_e, \mathbf{r}_p$  implicitly contained in  $m_e, m_p$  through relativistic effect (Sec 2.2) are not affected by this formal mapping. For the  $e, p$  relative motions (internal of a neutron) are of major concern in this paper, we shall hereafter work in the CM frame, i.e. in terms of the relative positions  $\mathbf{r}_e, \mathbf{r}_p, \mathbf{r}$  measured with respect to a set of relative coordinate axes  $x, y, z$  parallel with the  $X, Y, Z$  axes, and with an origin fixed at the CM (cf Fig 1b).

The partial–relative and relative velocities of the  $e, p$ , and the corresponding rotational angular momenta in the CM frame, in terms of the time  $t$ , follow as

$$\mathbf{v}_e = \frac{d\mathbf{r}_e}{dt} = \frac{m_p}{M}\mathbf{v}, \quad \mathbf{v}_p = \frac{d\mathbf{r}_p}{dt} = -\frac{m_e}{M}\mathbf{v}, \quad \mathbf{v} = \frac{d\mathbf{r}}{dt} = \mathbf{v}_e - \mathbf{v}_p; \quad (3)$$

$$\mathbf{J}_e = \mathbf{r}_e \times (m_e\mathbf{v}_e) = \frac{m_p}{M}\mathbf{J}, \quad \mathbf{J}_p = \mathbf{r}_p \times (m_p\mathbf{v}_p) = \frac{m_e}{M}\mathbf{J}, \quad \mathbf{J} = \mathbf{J}_e + \mathbf{J}_p = \mathbf{r} \times (\mathcal{M}\mathbf{v}) \quad (4)$$

From the relations (2g,h) between the distances  $\mathbf{r}_e, \mathbf{r}_p$  of  $e, p$  to the CM, and  $\mathbf{r}$  of  $e$  to  $p$  it follows that, by virtue how time in essence is defined, the local times  $t_e, t_p$  and the time  $t$  for light to traverse the distances  $\mathbf{r}_e, \mathbf{r}_p, \mathbf{r}$  at a constant velocity  $c$  are related as  $t_e = (m_p/M)t$ ,  $t_p = (m_e/M)t$ . The partial-relative velocities in terms of  $t_e, t_p$  are

$$\mathbf{v}'_e = d\mathbf{r}_e/dt_e = \mathbf{v}, \quad \mathbf{v}'_p = d\mathbf{r}_p/dt_p = -\mathbf{v}. \quad (5)$$

Denote  $f_t(e) = \frac{t}{t_e} = \frac{|d\mathbf{r}_e/dt|}{|d\mathbf{r}_e/dt_e|} = \frac{v'_e}{v_e}$ . Substituting  $t = f_t(e)t_e$  in (1a), setting  $\mathbf{R} = 0$ , we have  $m_e \frac{d^2\mathbf{r}_e}{d(f_t^2(e)t^2)} = m_e\mathbf{g}(t) + \mathbf{F}(t)$ , or  $m_e \frac{d^2\mathbf{r}_e}{dt^2} = m_e f_t^2(e)\mathbf{g}(t) + f_t^2(e)\mathbf{F}(t) = m_e\mathbf{g}(t_e) + \mathbf{F}(t_e)$ , recovering the original form of (1a) expressed by its local time  $t_e$  provided  $\mathbf{F}(t_e) = f_t^2(e)\mathbf{F}(t)$ ,  $\mathbf{g}(t_e) = f_t^2(e)\mathbf{g}(t)$ . Similarly a factor  $f_t(p) = \frac{t}{t_p} = \frac{v'_p}{v_p}$  will project (1b) to its original form expressed in  $t_p$ . The same projection factors, in the form of geometric mean  $f_t^2 = (f_t^2(e)f_t^2(p))^{1/2}$ , will be obtained through direct derivation of the magnetic force in Sec 4.

*2.2. Lorentz-Einstein transformations* The instantaneous rest frame fixed to each rotating particle,  $e, p, \mathcal{M}$  or  $M$ , may be regarded as an inertial frame for each differential rotation which is essentially linear. (For a complete macroscopic rotation, non-inertial frame effects present and will be included separately, see Eqs (11) vs (12) below and in turn Sec 2.4). Subsequently, the differentials of the space and time coordinates  $\mathbf{r}_e, t_e; \mathbf{r}_p, t_p; \mathbf{r}, t; \mathbf{R}$  in the CM frame and their counterparts  $\mathbf{r}_e^0, t_e^0; \mathbf{r}_p^0, t_p^0; \mathbf{r}^0, t^0; \mathbf{R}^0$  in the respective (instantaneous) rest frames are related by the Lorentz-Einstein transformations,

$$\begin{aligned} \gamma_e(d\mathbf{r}_e - \mathbf{v}'_e dt_e) &= d\mathbf{r}_e^0, \quad \gamma_e(dt_e - \frac{\mathbf{v}'_e \cdot d\mathbf{r}_e}{c'^2}) = dt_e^0; \quad \gamma_p(d\mathbf{r}_p - \mathbf{v}'_p dt_p) = d\mathbf{r}_p^0, \quad \gamma_p(dt_p - \frac{\mathbf{v}'_p \cdot d\mathbf{r}_p}{c'^2}) = dt_p^0; \\ \gamma(d\mathbf{r} - \mathbf{v} dt) &= d\mathbf{r}^0, \quad \gamma(dt - \frac{\mathbf{v} \cdot d\mathbf{r}}{c^2}) = dt^0; \quad \gamma_M(d\mathbf{R} - \mathbf{u}_M dt) = d\mathbf{R}^0; \end{aligned} \quad (6)$$

where  $\gamma_\alpha = (1 - v'_\alpha{}^2/c'^2)^{-1/2}$  ( $\alpha = e, p$ ),  $\gamma = (1 - v^2/c^2)^{-1/2}$ ,  $\gamma_M = (1 - u_M^2/c^2)^{-1/2}$ ;  $c' = d\mathbf{r}_{\alpha pht}/dt_\alpha = c = d\mathbf{r}_{pht}/dt$  is the light speed measured in the CM frame;  $\gamma_M, \gamma$  are the (effective) Lorentz factors of the fictitious particles of masses  $M, \mathcal{M}$  moving effectively at the velocities  $\mathbf{u}_M, \mathbf{v}$ , such that their dynamical consequence is the same as that due to the motions of  $m_e, m_p$  relative to the CM. In particular,  $\mathbf{u}_M$  needs be thought of as the speed of the CM relative to the  $e, p$ ; the CM is not moving relative to itself.

Transformations from the scalar distances  $r_e, r_p, R, r$  to  $r_e^0, r_p^0, R^0, r^0$  at fixed  $t$  (hence  $t_e, t_p$ ), from the time  $t$  to  $t^0$  at fixed  $\mathbf{r}$ , from the CM-frame masses  $m_e, m_p, M, \mathcal{M}$  to their respective rest-frame counterparts  $m_e^0, m_p^0, M^0 (= m_e^0 + m_p^0), \mathcal{M}^0 (= m_e^0 m_p^0 / M^0)$  follow as

$$\gamma_e r_e = r_e^0, \quad \gamma_p r_p = r_p^0, \quad \gamma_M R = R^0, \quad \gamma r = r^0; \quad \gamma t = t^0; \quad (7.1)$$

$$m_e = \gamma_e m_e^0, \quad m_p = \gamma_p m_p^0, \quad M = m_e + m_p = \gamma_M M^0, \quad \mathcal{M} = \gamma \mathcal{M}^0. \quad (7.2)$$

Using Eqs (7.2) for  $m_e, m_p, M, \mathcal{M}$  in (2b),(d) gives (8), and solving gives (9) below:

$$\gamma_M M^0 = \gamma_e m_e^0 + \gamma_p m_p^0, \quad \gamma_M \gamma = \gamma_e \gamma_p; \quad \text{or} \quad M^0 = m_e^\dagger + m_p^\dagger, \quad \text{where} \quad (8.1)$$

$$m_e^\dagger = \frac{m_e}{\gamma_M} = \gamma_e^\dagger m_e^0, \quad m_p^\dagger = \frac{m_p}{\gamma_M} = \gamma_p^\dagger m_p^0, \quad \gamma_e^\dagger = \frac{\gamma_e}{\gamma_M}, \quad \gamma_p^\dagger = \frac{\gamma_p}{\gamma_M}; \quad \gamma_e^\dagger \gamma_p^\dagger = \frac{\gamma_e \gamma_p}{\gamma_M^2} = \frac{\gamma}{\gamma_M} = \gamma^\dagger \quad (8.2)$$

$$\gamma_e = \frac{\gamma_M(M^0 \pm \Gamma)}{2m_e^0}, \quad \gamma_p = \frac{\gamma_M(M^0 \mp \Gamma)}{2m_p^0}, \quad \Gamma = \sqrt{(M^0)^2 - 4m_e^0 m_p^0 \gamma^\dagger}. \quad (9)$$

For (9) to have real solutions requires  $(M^0)^2 - 4m_e^0 m_p^0 \gamma^\dagger \geq 0$ , or  $\gamma^\dagger \leq (\gamma^\dagger)_{\max} = (M^0)^2 / 4m_e^0 m_p^0 = 459.556$ , where  $\gamma^\dagger = (\gamma^\dagger)_{\max}$  if  $\Gamma = 0$ , in which case  $\gamma_e = \gamma_M M^0 / 2m_e^0$ ,  $\gamma_p = \gamma_M M^0 / 2m_p^0 \simeq \frac{1}{2} \gamma_M$ ,  $m_e = m_p$ . In general  $m_e$  and  $m_p$  may not be equal. Let  $m_e = k m_p$ ; this combined with (9a) gives  $(m_e =) k m_p = \gamma_e m_e^0 = \frac{1}{2} \gamma_M (M^0 + \Gamma)$ . Dividing it by (9b) times  $m_p^0$ , i.e.  $(m_p =) \gamma_p m_p^0 = \frac{1}{2} \gamma_M (M^0 - \Gamma)$  gives (10a,b), and re-arranging (9c) gives (10c) below,

$$k = \frac{M^0 + \Gamma}{M^0 - \Gamma}, \quad \text{or} \quad \Gamma = \frac{(k-1)M^0}{k+1}; \quad \gamma^\dagger = \frac{(M^0)^2 - \Gamma^2}{4m_e^0 m_p^0} = \frac{k(M^0)^2}{(k+1)^2 m_e^0 m_p^0} \quad (10)$$

Substituting in these  $k = m_e/m_p = 1.3165$  from the solution for neutron magnetic moment (Sec 3) gives  $\Gamma = \frac{(1.3165-1)}{1.3165+1} 938.78(3) = 128.26(5)$  GeV, and  $\gamma^\dagger = 450.96(0)$ . Eqs (2g),(h) and (3a),(b) for this case become  $\mathbf{r}_e = \frac{\mathbf{r}}{k+1} = 0.43\mathbf{r}$ ,  $\mathbf{r}_p = -\frac{k\mathbf{r}}{k+1} = -0.57\mathbf{r}$ ;  $\mathbf{v}_e = 0.43\mathbf{v}$ ,  $\mathbf{v}_p = -0.57\mathbf{v}$  (cf Fig. 1c, right graph).  $k \gtrsim 1$  implies  $\gamma_e, \gamma_p \gg 1$ .

Multiplying  $\frac{\gamma_e m_e}{\gamma_e + 1}$  to the quadratics of Eq (3a), and  $\frac{\gamma_p m_p}{\gamma_p + 1}$  to that of (3a), adding, we obtain on the left side the total kinetic energy  $T_e + T_p$  of  $e, p$  measured in the CM frame and in time  $t$ ,

$$(T_e + T_p \equiv) \frac{\gamma_e m_e v_e^2}{\gamma_e + 1} + \frac{\gamma_p m_p v_p^2}{\gamma_p + 1} = \left[ \frac{\gamma_e m_p}{(\gamma_e + 1)M} + \frac{\gamma_p m_e}{(\gamma_p + 1)M} \right] \mathcal{M} v^2 (\equiv T) \quad (11.1)$$

$$\text{for } \gamma_e, \gamma_p \gg 1: \quad m_e v_e^2 + m_p v_p^2 = \mathcal{M} v^2 \quad (11.2)$$

The right side of (11.1) or (11.2) expresses the kinetic energy  $T$  of the reduced mass relative to the CM. Eq (11.1) or (11.2) expresses invariance of kinetic energy under the  $\mathbf{r}_e, \mathbf{r}_p$  to  $\mathbf{r}, \mathbf{R}$  coordinate transformation as described relative to CM frame and in time  $t$ . Performing similar operations to Eqs (5a,b) instead we obtain on the left side the total kinetic energy  $T'_e + T'_p$  of  $e, p$  measured in the CM frame but in their local times  $t_e, t_p$ ,

$$(T'_e + T'_p \equiv) \frac{\gamma_e m_e}{\gamma_e + 1} v_e'^2 + \frac{\gamma_p m_p}{\gamma_p + 1} v_p'^2 = \left[ \frac{\gamma_e m_e}{(\gamma_e + 1)M} + \frac{\gamma_p m_p}{(\gamma_p + 1)M} \right] M v^2 (\equiv T') \quad (12.1)$$

$$\text{for } \gamma_e, \gamma_p \gg 1: \quad m_e v_e'^2 + m_p v_p'^2 = (m_e + m_p) v^2 \quad (12.2)$$

The right side of (12.1) or (12.2) represents in effect the kinetic energy of the total mass at the CM relative to the  $e, p$  local space and time coordinates. Since  $m_e, m_p < M$ , so  $T'_e + T'_p > T_e + T_p$ . The difference  $(T'_e + T'_p) - (T_e + T_p)$  apparently represents a kinetic energy contribution from the non-inertial frame motion at  $\mathbf{r}_e, \mathbf{r}_p$  relative to the CM.

Unless specified otherwise we shall hereafter consider for simplicity a  $e, p$  system as a whole, i.e. its CM, being at rest in the lab frame. Provided further setting the coordinate origins of the CM and lab frames the same, i.e.  $\mathbf{R} = 0$ , the relativistic effects in the two frames are the same.

*2.3. On the neutron mass* For the CM (centre of mass) of the  $e, p$  system assumed at rest in the lab frame, naturally an observer in the lab frame will measure a rest total mass  $M^{\text{lab}} = M^0 = m_e^0 + m_p^0$  of the model neutron. In more elaborate terms, a measurement of the neutron mass in the laboratory is typically made in a specified say  $X$  direction over a macroscopic time interval  $\Delta t$  which is  $\gg 2\pi r/v$ , the rotation period of  $\mathcal{M}$  (Secs 2.4, 6). During  $\Delta t$ ,  $\mathbf{v} (= \mathbf{v}_e - \mathbf{v}_p)$  explores all directions with a zero average projection in the  $X$  direction. Hence

the relativistic augment in mass as measured along an instantaneous direction  $\mathbf{v}$  in the CM frame does not enter the mass  $M^{\text{lab}}$  measured in the lab frame. (This mass augment however evidently enters the interaction force or potential which has a constant magnitude so as to manifestly effectuate a bound  $e, p$  in stationary state irrespective of the direction of the  $e, p$  separation.)

A dually relevant example here is electron scattering by a target neutron. In respect to the internal dynamics of a target neutron, an incident electron  $e$  travelling in a fixed direction is as a (moving) observer in the lab frame. The incident  $e$  thus will see the rest (as contrasted to relativistic) masses of the  $e, p$  of the neutron. Moreover, the  $e, p$  of the neutron are fast rotating along circles of similar radii about their CM and thus about equally exposed to the incident  $e$ . So in terms of exposure frequency, the  $e, p$  would equally probably scatter with the incident  $e$ , through electro and magnetic potentials and naturally at their contracted radii  $a_e, a_p$ . The scattering potential from the proton  $p$  of the neutron, on the other hand, would dominate because of its much heavier rest mass, which for the electrostatic part at least is attractive. Incidentally, the experimentally measured electron-neutron scattering length is negative and suggests an attractive scattering potential.

The (very large)  $e, p$  interaction potential fields within the neutron, on the other hand, are liable to (considerably) modify the vacuum potential surrounding the  $e, p$  charges; the effect would be particularly large given the  $e, p$  separation distance  $10^{-18}$  m (Sec 6) here is comparable with the inter-vacuum distance based on the "vacuonic vacuum structure"<sup>a</sup>. This would consequently further modify the  $e, p$  particles' rest masses, in terms of the IED model<sup>b</sup>, produced as their generating charges move through this modified vacuum. (*a, b*: see the author's earlier published work). The above gives a qualitative account for the (order of MeV) larger neutron rest mass over the sum of the  $e, p$  rest masses; this difference is relatively small and ignored where in question throughout this paper.

*2.4. Eigenvalue equations. Orbital and precessional angular momenta. Antineutrino* In the absence of applied force and omitting the very weak gravity,  $M$  is free and hence not directly subject to quantisation condition. We thus need only to establish the relativistic Schrödinger or Klein-Gordon equation (KGE) for the mass  $\mathcal{M}$ , in terms of the spherical polar coordinates  $r, \vartheta, \phi$  transformed from the coordinates  $x, y, z$ , without regard to the associated non-inertial frame effect for the present. The KGE has the usual form  $[(E_{\text{tot}})_{op} - V]^2 - \mathcal{M}^0 c^4 - (p^2)_{op} c^2] \psi_{\text{tot}} = 0$ . Since the mass  $\mathcal{M}$  under consideration is moving at velocity exceedingly close to  $c$  such that its rest-mass energy is negligibly small compared to its kinetic energy (Sec 6), more relevant to it is the square-root (SQR) form of the KGE:  $\mathcal{H}_{op} \psi = \mathcal{H} \psi$ , where  $\mathcal{H}_{op} = ((E_{\text{tot}})_{op} - V) - \mathcal{M}^0 c^2 + V = \frac{\gamma(p^2)_{op}}{(\gamma+1)\mathcal{M}} + V$  is the Hamiltonian operator associated with the kinetic motion of  $\mathcal{M}$ ;  $(p^2)_{op} = (p_r^2)_{op} + \frac{(\mathcal{J}^2)_{op}}{\mathcal{M} r^2}$ ;  $(p_r^2)_{op}$  and  $(\mathcal{J}^2)_{op}$  are the squared radial and orbital angular momentum operators. For the  $e, p$  interaction potential  $V$  being central (Sec 4), hence  $V(\mathbf{r}) = V(r)$ , the wave function of  $\mathcal{M}$ ,  $\psi(r, \vartheta, \phi)$ , may be written as  $\psi = \mathcal{R}(r)\mathcal{Y}(\vartheta, \phi)$ . And the SQR-KGE separates into two eigen value equations,

$$\left[ -\frac{\gamma \hbar^2}{(\gamma+1)\mathcal{M} r^2} \frac{\partial}{\partial r} \left( r^2 \frac{\partial}{\partial r} \right) + \frac{\gamma l(l+1) \hbar^2}{(\gamma+1)\mathcal{M} r^2} + V(r) \right] \mathcal{R}(r) = \mathcal{H} \mathcal{R}(r) \quad (13)$$

$$(\mathcal{J}^2)_{op} \mathcal{Y}(\vartheta, \phi) = \mathcal{J}^2 \mathcal{Y}(\vartheta, \phi), \quad (\mathcal{J}^2)_{op} = -\hbar^2 \left( \frac{\partial^2}{\partial \vartheta^2} + \cot \vartheta \frac{\partial}{\partial \vartheta} + \frac{1}{\sin^2 \vartheta} \frac{\partial^2}{\partial \phi^2} \right). \quad (14)$$

(14) may be solved without  $V(r)$  being explicitly known. The eigen functions are the spherical harmonics,  $\mathcal{Y}_l^{m_l} = C_l^{m_l} P_l^{m_l}(\cos \vartheta) e^{im_l \phi}$ . The square-root eigen values and their  $z$  components are

$$\mathcal{J}_l = |\mathbf{r}_l \times (\mathcal{M} \mathbf{v}_{t_l})| = \sqrt{l(l+1)} \hbar, \quad \mathcal{J}_{z m_l} = \mathcal{J}_l \cos \vartheta_{m_l} = m_l \hbar, \quad l = 0, 1, \dots; m_l = 0, \dots, \mp l. \quad (15)$$

Based on the semiclassical expression  $\mathbf{r}_l \times (\mathcal{M}\mathbf{v}_{tl})$ , the particle of mass  $\mathcal{M}$  in  $l$ th state executes an orbital angular motion along a circular orbit  $l$  of radius vector  $\mathbf{r}_l$  at a tangential velocity  $\mathbf{v}_{tl} = \boldsymbol{\omega}_o \times \mathbf{r}_l$ ,  $\boldsymbol{\omega}_o = \mathbf{r}_l \times \mathbf{v}_{tl}/r_l^2$ ;  $\mathbf{r}_l \equiv \mathbf{r}_n$ , where  $n$  is the principal quantum number,  $l = 0, 1, \dots, n-1$ . The normal of the orbital plane, or the axis of rotation  $\mathbf{n}_o$  passes through the CM and is at a quantised angle  $\vartheta_{m_l}$  to the  $z$  axis.

Owing to their having a finite (radial) acceleration,  $\mathbf{a}_l = -|d^2\mathbf{r}_l/dt^2|(\mathbf{r}_l/r_l)$ , as a well-known non-inertial frame effect the  $e, p$  in addition execute a Thomas precession (TP), with an instantaneous angular velocity  $\boldsymbol{\omega}_{TP}$  and angular momentum  $\mathbf{J}_{TP} = r_l^2\mathcal{M}\boldsymbol{\omega}_{TP}$  here.  $\boldsymbol{\omega}_{TP} = \frac{\gamma^2}{(\gamma+1)} \frac{\mathbf{a}_l \times \mathbf{v}_{tl}}{c^2}$  as originally derived by LH Thomas (1927), and as may be alternatively derived directly based on infinitesimal Newtonian inertial-frame (hence linear) motion plus a Newtonian acceleration each in relativistic terms here (internal work).  $\boldsymbol{\omega}_{TP}$  is in the instantaneous direction  $\mathbf{a}_l \times \mathbf{v}_{tl} \propto -\mathbf{r}_l \times \mathbf{v}_{tl} = -\mathcal{J}_l/\mathcal{M}$ , i.e. opposite to  $\mathcal{J}_l$ , describing an instantaneous rotation in opposite sense to the orbital angular motion underlining  $\mathcal{J}_l$ . For a quantum system as the bound  $e, p$  here, the  $z$  component of  $\mathbf{J}_{TP}$ ,  $J_{TPz}$ , will be necessarily constrained such that both the space quantisation conditions (15) above and (16) below are met.

The total, precessional-orbital angular momentum  $J_j (= |\mathcal{J}_l - \mathbf{J}_{TP}|)$  and its  $z$  component  $J_{zm_j} (= \mathcal{J}_{zm_l} - J_{TPz} = J_j \cos \theta_{m_j} \hat{z})$  are given according to the quantum vector addition model as

$$J_j = |\mathcal{J}_l - \mathbf{J}_{TP}| = |\mathbf{r}_{lj} \times (\mathcal{M}\mathbf{v}_j)| = r_l \mathcal{M} v_j = \sqrt{j(j+1)} \hbar, \quad j = l - l_{TP} = 0, \frac{1}{2}, 1, \frac{3}{2}, \dots \quad (16.1)$$

$$J_{zm_j} = J_j \cos \theta_{m_j} = \mp J_j \cos \theta_j = m_j \hbar, \quad m_j = \mp j, \quad (16.2)$$

where the permitted  $j$  values are results of the general solutions of the quantum commutation relation for the angular momentum  $\mathbf{J}$  here,  $\mathbf{J} \times \mathbf{J} = i\hbar\mathbf{J}$ .  $\mathbf{r}_{lj} = r_l \hat{r}_{lj}$  is the quantised radius vector of the instantaneous circular orbit  $l$  of a normal or axis of rotation  $\mathbf{n}$ ;  $\mathbf{n}$  is at a fixed angle  $\theta_{m_j} = \arccos(J_{zm_j}/J_j)$  to the  $z$  axis and rotates about the  $z$  axis at the angular velocity  $\boldsymbol{\omega}_{TPz}$ , whence the Thomas precession; see Fig 1b. The magnitude of  $\mathbf{r}_{lj}$ ,  $|\mathbf{r}_{lj}| = r_l (= r_n|_{n=l+1})$  is unchanged subjected to the quantum equation (15a).  $\mathbf{v}_j = \boldsymbol{\omega} \times \mathbf{r}_{lj}$ ;  $\boldsymbol{\omega} = \mathbf{r}_{lj} \times \mathbf{v}_j/r_l^2 = (\boldsymbol{\omega}_o - \boldsymbol{\omega}_{TP})\hat{\boldsymbol{\omega}}$  is the precessional-orbital angular velocity. For facilitating later discussion we attach as in Fig 1b the axes  $x', y', z'$  to the instantaneous rest frame of the precessional orbit  $l$ , with their origin fixed at the CM, hence coinciding with that of  $x, y, z$ . So the  $x', y', z'$  axes precess about the  $z$  axis at the angular velocity  $\boldsymbol{\omega}_{TPz}$ , in such a way that the  $z'$  axis is at fixed angle  $\theta_j$  to the  $z$  axis and along the  $\mathbf{n}$  direction; the  $x'$  axis is always at angle  $\theta_j$  from (its projection  $x'_{xy}$  in) the  $xy$  plane and always along the  $\mathbf{r}_{lj}$  direction; the  $y'$  axis lies in the  $xy$  plane and rotates about the  $z$  axis. And we attach the  $x'', y'', z''$  axes to the instantaneous rest frame of the precessing-orbiting  $e, p$  particles with an origin fixed at the CM too, and the  $z''$  axis coinciding with  $z'$ ; the  $x'', y''$  axes lie in the  $x'y'$  plane and are rotating about the CM at an angular velocity  $\omega_o + \omega_{TP}$  (for the  $m_j = -j$  state) in clockwise sense relative to  $x', y'$ , with the  $x''$  axis (shown in Fig 1b) lying along the line joining  $e, p$ .

From Eq (16.1b), it follows that the permitted  $l_{TP}$  values are uniquely specified once  $l, j$  are specified according to (15),(16): For  $l = 0$ , only  $l_{TP} = 0$  is permitted; and  $j = l = 0$ . This gives an  $e, p$  system not magnetically bound at a separation of the order  $10^{-18}$  m (see further Sec 4), and would in principle render a hydrogen system only. For any non zero, integer  $l$  values  $l = 1, 2, \dots$ ,  $l_{TP} = 0$  is permitted formally by (16.1) but is however unphysical because of the so implied absence of Thomas precession.  $l_{TP} = \frac{1}{2}$  is therefore the smallest finite and hence physical value which is also permitted based on the quantum solutions for  $l, j$ . Moreover,  $l_{TP} = \frac{1}{2}$  is itself a solution for  $\mathbf{J}_{TPz}$  to separately satisfy the quantum commutation relation  $\mathbf{J}_{TPz} \times \mathbf{J}_{TPz} = i\hbar\mathbf{J}_{TPz}$ ; this establishes a condition for the carrier of  $\mathbf{J}_{TPz}$ , the neutral rotational energy flux (to be identified as the antineutrino) to be created or emitted as a quantum particle.



For the permitted  $l$  and  $l_{TP} = \frac{1}{2}$ , Eqs (16) are written as

$$J_j = r_l \mathcal{M} v_j = \sqrt{j(j+1)} \hbar = \frac{\sqrt{(4l^2-1)} \hbar}{2}, \quad j = l - \frac{1}{2} = \frac{1}{2}, \frac{3}{2}, \dots; \quad (16.1)'$$

$$J_{zm_j} = J_j \cos \theta_{m_j} = m_j \hbar = (\mp |m_l| \pm \frac{1}{2}) \hbar, \quad m_j = \mp j = \mp |m_l| \pm \frac{1}{2} = \mp \frac{1}{2}, \dots, \mp j, \quad (16.2)'$$

where  $\cos \theta_{m_j} = \frac{J_{zm_j}}{J_j} = \frac{2l-1}{\sqrt{4l^2-1}}$ . For  $j = \frac{1}{2}$ ,  $m_j = \mp \frac{1}{2}$ :

$$J_{\frac{1}{2}} = |\mathbf{r}_{1\frac{1}{2}} \times (\mathcal{M} \mathbf{v}_{\frac{1}{2}})| = r_1 \mathcal{M} v_{\frac{1}{2}} = \frac{\sqrt{3} \hbar}{2}, \quad J_{z\mp\frac{1}{2}} = r_1 \mathcal{M} v_{\frac{1}{2}} \cos \theta_{\mp\frac{1}{2}} = \mp \frac{\hbar}{2}; \quad (17)$$

$\cos \theta_{\frac{1}{2}} = J_{z\frac{1}{2}}/J_{\frac{1}{2}} = 1/\sqrt{3}$ ;  $\theta_{\frac{1}{2}} = \arccos(1/\sqrt{3}) = 54.7^\circ$ . The  $j = \frac{1}{2}$  ( $l = 1$ ) states describe a ground-state neutron (Secs 3, 4). Eq (17a) thus gives the  $e, p$  relative precessional-orbital angular momentum internal of the neutron, and (17b) the two possible  $z$  components associated with a minimum-energy ( $m_j = -\frac{1}{2}$ ) and excitation ( $m_j = \frac{1}{2}$ ) state in an applied magnetic field in the  $+z$  direction (see Sec 3). The precessing circular orbit of the mass  $\mathcal{M}$  has the quantised radius vector  $\mathbf{r}_{1\frac{1}{2}}$  about the CM in the  $x'y'$  plane. For the  $m_j = -\frac{1}{2}$  state, the normal  $\mathbf{n}$  of the rotation plane, and hence  $\mathbf{J}_{\frac{1}{2}}$ , is at angle  $\theta_{-\frac{1}{2}} = \pi - \theta_{\frac{1}{2}}$  to the  $z$  axis; the rotation is in clockwise sense, as in Fig 1b. And conversely for  $m_j = \frac{1}{2}$ . For the next orbital,  $j = \frac{3}{2}$  ( $l = 2$ ),  $J_{z\frac{3}{2}}/J_{\frac{3}{2}} = 3/\sqrt{15}$ ,  $\theta_{\frac{3}{2}} = 39.2^\circ$ .

For the neutron existing (in zero applied field) only in a single non-degenerate state  $j = l - \frac{1}{2} = \frac{1}{2}$  and presuming that, in terms of the SQR-KGE here, energies of different  $l$  and same  $n$  are degenerate, then  $N$  (the radial degree of freedom) = 0 and  $n = N + l + 1 = 0 + l + 1 = 2$ . So  $T_{rl}|_{l=n-1=1} = 0$ ; and the total kinetic energy of  $\mathcal{M}$  is, with  $J_{\frac{1}{2}}^2 (= (\mathcal{J}_1 - J_{TPz})^2)$  for  $\mathcal{J}_1^2$ ,

$T_{\frac{1}{2}} = T_{t\frac{1}{2}} = \frac{\gamma \mathcal{M} v_{\frac{1}{2}}^2}{(\gamma+1)} = \frac{\gamma J_{\frac{1}{2}}^2}{(\gamma+1) \mathcal{M} r_1^2} = \frac{3\gamma \hbar^2 M}{4(\gamma+1)m_e m_p r_1^2}$ . Accordingly, the eigen energy (Hamiltonian)  $H_j = T_j + V_j$ , in place of  $\mathcal{H}_{l=n-1} = \mathcal{J}_{l=n-1} + V_{l=n-1}$  (where  $\mathcal{H}_{l=n-1} \equiv \mathcal{H}_n$ , etc.), may be directly computed from the sum of the  $T_j$  given above (in place of  $\mathcal{J}_{l=n-1}$ ) and the  $V_j$  to be derived in Sec 4, without formally solving the radial differential equation (13).

The  $e, p$  relative precessional-orbital motion, or more precisely the propagation of the matter waves  $\psi_e, \psi_p$  of the  $e, p$  particles relative to one another or alternatively of the matter wave  $\psi$  of  $\mathcal{M}$ , is associated with a neutral rotational kinetic energy flux, or vortex, on disregarding their charges and also their rest-mass energies. This vortex entity carries a spin angular momentum with a  $z$  component equal to one unit of half-integer quantum  $J_{z\mp\frac{1}{2}} = \mp \frac{1}{2} \hbar$ , has apparently a positive helicity, and therefore resembles directly an antineutrino ( $\bar{\nu}_e$ ) confined within the neutron; see further Sec 5. Accordingly the  $z$ -component spin angular momenta of  $\bar{\nu}_e$  are

$$S_{\bar{\nu}_e z} = J_{z\mp\frac{1}{2}} = \mp \frac{1}{2} \hbar = \mp s_{\bar{\nu}_e} \hbar, \quad s_{\bar{\nu}_e} = \frac{1}{2}. \quad (18)$$

### 3. $e, p$ system magnetic structure. Neutron magnetic moment, (effective) spin

*3.1  $e, p$  spins and magnetic moments. Neutron internal spin configurations.* *Total spin* Either particle  $\alpha = e$  or  $p$  has an intrinsic spin  $s_\alpha = \frac{1}{2}$ , spin angular momentum  $S_\alpha = \sqrt{s_\alpha(s_\alpha+1)} \hbar = \frac{\sqrt{3}}{2} \hbar$  about a spin axis  $\mathbf{n}_\alpha$  passing through  $\mathbf{r}_\alpha$ , and  $z$  component  $S_{\alpha z} = S_\alpha \cos \theta_\alpha^s = s_\alpha \hbar$ . For the spin up state as in Fig 1a,  $\cos \theta_\alpha^s = S_{\alpha z}/S_\alpha = 1/\sqrt{3}$ ; the spin axis  $\mathbf{n}_\alpha$  is at fixed angle  $\theta_\alpha^s = 54.73^\circ$  to a  $z_\alpha^s$  axis parallel with  $z$  and passing through  $\mathbf{r}_\alpha$ . Certain external, random environmental in the case of zero applied, magnetic field would always present and thus define the (instantaneous)  $z$  direction here. For computing the magnetic field produced by the spin motion of one particle  $\alpha$  on the other particle ( $\alpha'$ ),  $\mathbf{B}_\alpha^s$  (Eq 29b for  $\alpha = p$ , Sec 4) at a separation  $r_l$  comparable to the sizes of their charges (Secs. 4, 6), it is appropriate

to treat the  $e, p$  charges as extended objects, firstly simply as spheres of radii  $a_e, a_p$  with their mass and charge densities specified in the following way. We assume that the mass  $m_\alpha$  of either particle  $\alpha$  is distributed predominantly within its charge (and thus by a negligible amount in its wave field), with a volume density  $\rho_\alpha(\boldsymbol{\xi}_\alpha)$  at a distance  $\boldsymbol{\xi}_\alpha$  from  $\mathbf{r}_\alpha$ ;  $dm_\alpha = m_\alpha \rho_\alpha(\boldsymbol{\xi}_\alpha) d^3\xi_\alpha$  thus is a mass element at  $\boldsymbol{\xi}_\alpha$ . So  $S_\alpha$  is given rise to by the angular motion of the sphere about  $\mathbf{n}_\alpha$  at the angular velocity  $\omega_\alpha^s = d\phi_\alpha^s/dt_\alpha$ , tangential velocity  $v_\alpha^s = a_\alpha \omega_\alpha^s$  as,

$$S_\alpha = m_\alpha \int |\boldsymbol{\xi}_\alpha \times \mathbf{v}_\alpha^s| \rho_\alpha(\boldsymbol{\xi}_\alpha) d^3\xi_\alpha = \frac{1}{g_\alpha} a_\alpha^2 \omega_\alpha^s m_\alpha = \frac{\sqrt{3}}{2} \hbar; \quad S_{\alpha z} = \frac{1}{g_\alpha} a_\alpha^2 m_\alpha \omega_\alpha^s \cos \theta_\alpha^s = \frac{1}{2} \hbar \quad (19)$$

where  $g_\alpha$  is the Lande  $g$  factor of particle  $\alpha$ . And the charge  $q_\alpha$  of either particle  $\alpha$  is distributed along a circular loop of radius  $a_\alpha$  with a normal parallel with  $\mathbf{n}_\alpha$ . The spin (dipole) magnetic moment  $\mu_\alpha^s$  of particle  $\alpha$  is accordingly produced by the current loop of charge  $q_\alpha$ , area  $\pi a_\alpha^2$ , and angular velocity  $\omega_\alpha^s$  in the  $\mp S_\alpha$  direction for  $q_\alpha = \mp e$ . The  $z$  components, written for  $e, p$  explicitly, are

$$\mu_{ez}^s = e \frac{\omega_e^s}{2\pi} \pi a_e^2 \cos(\pi - \theta_e^s) = -\frac{g_e e S_{ez}}{2m_e} = -\frac{g_e e \hbar}{4m_e}; \quad \mu_{pz}^s = \frac{g_p e S_{pz}}{2m_p} = \frac{g_p e \hbar}{4m_p} \quad (20)$$

For either particle  $\alpha$ , besides the  $z_\alpha^s$  above we further specify the local axes  $x_\alpha^s, y_\alpha^s$  to be parallel with the  $x, y$  but with an origin located at  $\mathbf{r}_\alpha$ . Its spin axis  $\mathbf{n}_\alpha$  as projected in this  $x_\alpha^s y_\alpha^s$  plane is unspecified in orientation according to the uncertainty principle, and in the external magnetic field in  $z$  direction would rotate about the  $z_\alpha^s$  axis. Accordingly the direction of  $\mathbf{v}_\alpha^s$  at any fixed point on the current loop varies over time as the current loop precesses. Since the  $z$  component  $S_{\alpha z}$  of  $S_\alpha$  is a constant (Eq 19b), the projection of  $\mathbf{v}_\alpha^s$  in the  $x_\alpha^s y_\alpha^s$  plane is a constant,  $v_{\alpha xy}^s = (a_\alpha \cos \theta_\alpha^s) \omega_\alpha^s = v_\alpha^s \cos \theta_\alpha^s$ ; this gives also the time average of  $\mathbf{v}_\alpha^s$ , for the projection of  $\mathbf{v}_\alpha^s$  in  $z$  direction averages to zero over time. For deriving an effective algebraic equation for the magnetic field produced by the spin current loop (Sec 4), the distinct symmetry property of the system will be utilised to further reduce the system to a two point half-charge representation (Appendix A).

*3.2  $e, p$  system spin configuration. Total spin angular momentum* For the  $e, p$  to be in a bound, minimum (internal magnetic) energy state (Sec 4), apart from  $j = \frac{1}{2}$ ,  $m_j = \mp \frac{1}{2}$  (Sec 2.4),  $S_{ez}, S_{pz}$  need be parallel mutually and each antiparallel to  $J_{zm_j}$  (Figs 1a,b; 2a,b).  $S_{ez}, S_{pz}, J_{zm_j}$  may therefore assume two possible configurations

$$(i) \quad S_{ez} = \frac{1}{2} \hbar, \quad S_{pz} = \frac{1}{2} \hbar, \quad J_{z-\frac{1}{2}} = -\frac{1}{2} \hbar; \quad (ii) \quad S_{ez} = -\frac{1}{2} \hbar, \quad S_{pz} = -\frac{1}{2} \hbar, \quad J_{z\frac{1}{2}} = \frac{1}{2} \hbar \quad (21)$$

as shown in Figs 2a,b.

Based on the usual vector addition model, the total angular momentum of the  $e, p$  system, denoted by  $\mathcal{J}_{j_n}$ , in the precessional-orbital state  $j = \frac{1}{2}$  are

$$\mathcal{J}_{j_n} = \sqrt{j_n(j_n + 1)} \hbar = \frac{\sqrt{3}}{2} \hbar, \quad j_n = (s_e + s_p) - j = \left(\frac{1}{2} + \frac{1}{2}\right) - \frac{1}{2} = \frac{1}{2} \quad (22)$$

Its  $z$  components  $\mathcal{J}_{zm_{j_n}}$  for the  $m_{j_n} = \pm j_n$  states are

$$\mathcal{J}_{z\pm\frac{1}{2}} = (S_{pz} + S_{ez})_{\text{down}}^{up} + J_{z\mp\frac{1}{2}} = \left[\pm\left(\frac{1}{2} + \frac{1}{2}\right) \mp \frac{1}{2}\right] \hbar = \pm \frac{1}{2} \hbar. \quad (23)$$

*3.3 Total magnetic moment* The differing  $g$  factors and potentially also asymmetric relative positions of  $e, p$  suggest an asymmetric internal magnetic structure of the  $e, p$  system. One thus expects a total magnetic moment which is not simply related to  $\mathcal{J}_{zm_{j_n}}$  of Eqs (23) as for a simple particle; nor would it be zero as implied by its zero net charge as both given by the

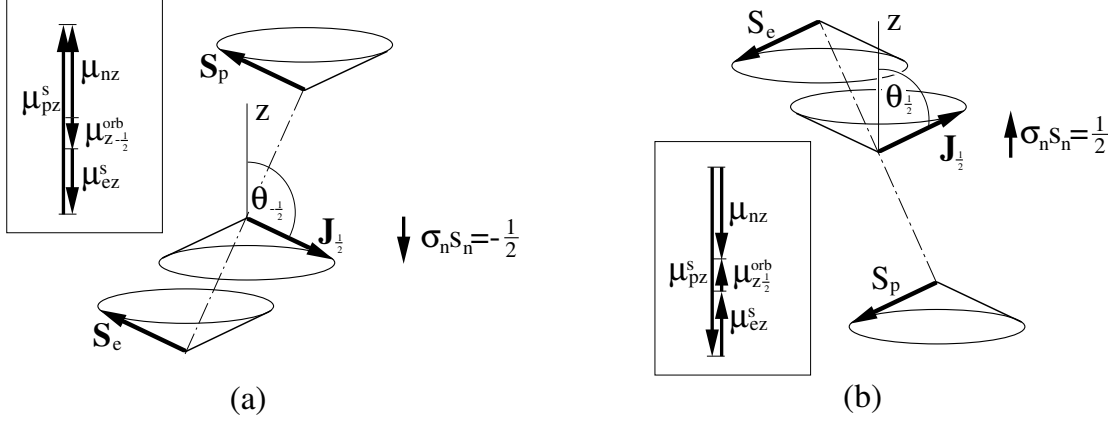


**Figure 2.** Internal angular momenta  $S_e, S_p, J_{m_j}$  of the model neutron with the internal spin configurations (a)  $s_e, s_p, m_j = \frac{1}{2}, \frac{1}{2}, -\frac{1}{2}$  in effective spin down state  $s_n \sigma_n = m_j = -\frac{1}{2}$ , and (b)  $s_e, s_p, m_j = -\frac{1}{2}, -\frac{1}{2}, \frac{1}{2}$  in effective up state  $\sigma_n s_n = m_j = \frac{1}{2}$ . Insets in (a),(b): the corresponding neutron magnetic moments  $\mu_{nz}$  given by respective vector sums of internal moments projected in  $z$  direction.

direct sum of the  $e, p$  charges here and from experimental observation. We shall find the total magnetic moment based directly on vector addition of the individual magnetic moments along  $z$  direction below. For the spin configuration (i) of Eqs (21), the  $z$ -component total magnetic moment of the  $e, p$  spins is the vector sum

$$\mu_z^s = \mu_{pz}^s + \mu_{ez}^s = \frac{g_p e S_{pz}}{2m_p} - \frac{g_e e S_{ez}}{2m_e} = \left(g_p - \frac{g_e}{k}\right) \frac{e S_{pz}}{2m_p}, \quad (24)$$

where the last of Eqs (24) is given after substituting  $m_e = k m_p$  (as in Sec 2.2) and  $S_{ez} = S_{pz}$ .  $k$  may in general differ from 1. So the relative precessional-orbital motion may contribute a finite moment given by the vector sum, for the case (i) or  $m_j = -\frac{1}{2}$ ,

$$\mu_{z-\frac{1}{2}}^{orb} = \frac{e J_{pz-\frac{1}{2}}}{2m_p} - \frac{e J_{ez-\frac{1}{2}}}{2m_e} = \frac{e \left(\frac{m_e}{M}\right) J_{z-\frac{1}{2}}}{2m_p} - \frac{e \left(\frac{m_p}{M}\right) J_{z-\frac{1}{2}}}{2m_e} = \left(\frac{k-1}{k}\right) \frac{e J_{z-\frac{1}{2}}}{2m_p} \quad (25)$$

where  $J_{\alpha z m_j}$  are given by the  $z$ -projections of  $J_\alpha$  of Eqs (4a,b);  $g = 1$  is assumed. The total  $z$ -component magnetic moment of the  $e, p$  system is the vector sum

$$\mu_{z-\frac{1}{2}\phi} = \mu_z^s + \mu_{z-\frac{1}{2}}^{orb} = \left(g_p - \frac{g_e}{k}\right) \frac{e(-J_{z-\frac{1}{2}})}{2m_p} + \left(\frac{k-1}{k}\right) \frac{e J_{z-\frac{1}{2}}}{2m_p} = -g_n \frac{e J_{z-\frac{1}{2}}}{2m_p}, \quad (26a)$$

$$g_n = g_p - \frac{g_e}{k} - \frac{k-1}{k} \quad (26b)$$

where in the expression of  $\mu_z^s$  we substituted  $S_{pz} = -J_{z-\frac{1}{2}}$ ;  $J_{z m_j}$ , instead of  $\mathcal{J}_{z m_j n}$ , is used for reason to be explained below. The subscript  $\phi$  indicates that the total  $\mu_{z-\frac{1}{2}\phi}$ , as the  $\mu_{pz}^s, \mu_{ez}^s$  and  $\mu_{z-\frac{1}{2}}^{orb}$ , is as directly probed by a detector placed at the CM relative to which the  $e, p$  are moving in the  $\mathbf{v}_e, \mathbf{v}_p$  or  $\phi$  directions, in which case the relativistic masses  $m_e, m_p$  in Eq (26a) remain physical.

An experimenter (as an external observer) in the laboratory on the other hand commonly probes the neutron magnetic moment by applying a magnetic field to turn the moment along the  $\theta$  direction, typically at a speed  $u_\theta \ll c$ . This is to turn the  $e, p$  system as a whole

here, or manifestly the  $e, p$  precessional-orbital plane about the  $y'$  axis along the  $\theta$  direction in the  $x'z'$  plane, i.e. in a direction perpendicular to  $\mathbf{v}_e, \mathbf{v}_p$ . So immediately for the proton  $\gamma_{p\theta} = (1 - u_{p\theta}^2/c^2)^{-1/2} \simeq 1$ ,  $m_p(u_{p\theta}) = \gamma_{p\theta} m_p^0 \simeq m_p^0$ ; the proton dominates the turning process because of its much larger rest-mass moment of inertia. The electron can only be turned in the same rigid precessional-orbital plane as the proton in a bound relativistic dynamic process, its mass (hence moment of inertia) must therefore manifestly be weighed by the same factor  $k$  as in this relativistic process, i.e. as  $m_e = km_p$ , not as  $m_e^0$ . The only means of correctly carrying the factor  $k$  through to the experimenter's result (Eq 27 below) is to convert  $m_e$  to  $km_p$  before transforming to Eq (27), as has been done in (26a). Substituting  $m_p^0$  in place of  $m_p$  in the last of Eqs (26a), and accordingly  $\mu_{z-\frac{1}{2}}$  in place of  $\mu_{z-\frac{1}{2}\phi}$ , gives therefore the  $z$ -component magnetic moment of the model neutron,  $\mu_{nz}$ , as probed by the experimenter, for the  $m_j = -\frac{1}{2}$  state

$$\mu_{nz}(m_j = -\frac{1}{2}) = \mu_{z-\frac{1}{2}} = -\frac{g_n e J_{z-\frac{1}{2}}}{2m_p(u_{p\theta})} = -\frac{g_n e J_{z-\frac{1}{2}}}{2m_p^0} = \frac{g_n e \hbar}{4m_p^0} = \frac{1}{2} g_n \mu_N, \quad (27)$$

where  $\mu_N = \frac{e\hbar}{2m_p^0}$  (the nuclear magneton). Similarly for the  $m_j = \frac{1}{2}$  state we obtain  $\mu_{nz}(m_j = \frac{1}{2}) = \mu_{z\frac{1}{2}} = -g_n e J_{z\frac{1}{2}}/2m_p^0 = -\frac{1}{2} g_n \mu_N$ .  $g_n$  represents the  $g$  factor of the model neutron. Equating  $g_n$  of (26b) with the experimental value  $g_n^{exp} = 3.8261$ , and using the experimental  $g$  values of  $e, p$ ,  $g_p = 5.5856$ ,  $g_e = 2$ , numerical solution for  $k$  is obtained as  $k = 1.3165$ . According to (27) or (26a),  $\mu_{z-\frac{1}{2}} > 0$ , i.e.  $\mu_{z-\frac{1}{2}}$  points in the  $+z$  direction, and is in the opposite direction to  $J_{z-\frac{1}{2}}$  (Fig 2a). And  $\mu_{z\frac{1}{2}} < 0$  (Fig 2b). Clearly, the magnetic moment of the model neutron is dominated by the proton spin magnetic moment because of the asymmetrically much larger  $g_p$  over  $g_e$ . From  $k > 1$  and hence  $m_e > m_p$ ,  $r_p > r_e$  (by a small amount each), it follows that  $\mu_{z-\frac{1}{2}}^{orb}$  points in the  $-z$  direction, adding a negative but small term to  $\mu_{z-\frac{1}{2}}$ .

**3.4 Effective spin of the neutron** In an applied magnetic field say  $\mathbf{B}_0$  in  $+z$  direction, the magnetic-interaction energy of the  $e, p$  system with the field is  $U_j = -\boldsymbol{\mu}_j \cdot \mathbf{B}_0 = -\mu_{zm_j} B_0$ .  $U_j < 0$  for the spin configuration (i) of Eqs (21) or the  $m_j = -\frac{1}{2}$  state, and  $U_j > 0$  for (ii) or the  $m_j = \frac{1}{2}$  state. That is, (i) or  $m_j = -\frac{1}{2}$  corresponds to the minimum-energy state and (ii) or  $m_j = \frac{1}{2}$  the excited state in the applied field. A transition from the minimum-energy to excited state corresponds to a flip of the spin-configuration (i) to (ii) of the bound  $e, p$  system as a whole, which is dictated, and thus manifested by the flip of the precessional-orbital plane from the  $m_j = -\frac{1}{2}$  state to  $m_j = +\frac{1}{2}$ . In other terms,  $\mu_{z-\frac{1}{2}}$  is as if produced by a negative charged current loop in spin up state, or alternatively by a positively charged current loop in spin down state. In so far as the total magnetic moment of the  $e, p$  system as a whole, whence the model neutron, is probed, it is therefore physical to assign to it an effective spin  $s_n$  and spin vector  $\sigma_n$ , corresponding directly to the  $j$  and  $m_j = \mp j$  values (rather than the  $j_n$  and  $m_{j_n}$ ). So the effective neutron spin angular momentum  $S_n$ , its  $z$  components  $S_{nz}$ , and accordingly  $\mu_{zm_j}$  in relation with  $S_{nz}$ , given by substituting  $S_{nz}$  for  $J_{zm_j}$  in (27), are

$$S_n = \sqrt{s_n(s_n + 1)} \hbar \equiv J_j = \frac{\sqrt{3}}{2} \hbar, \quad s_n = j = \frac{1}{2}; \quad S_{nz} = \sigma_n s_n \hbar \equiv J_{zm_j} = m_j \hbar = \mp \frac{1}{2} \hbar, \\ \sigma_n = \mp 1 \text{ (for } m_j = \mp \frac{1}{2}\text{);} \quad \mu_{nz} = -\frac{g_n e S_{nz}}{2m_p^0} = -\frac{g_n \sigma_n s_n e \hbar}{2m_p^0} \equiv \mu_{zm_j} = \pm \frac{g_n e \hbar}{4m_p^0} \quad (28)$$

Notice that for either spin configuration the  $S_n, S_{zn}$  are equal to  $\mathcal{I}_{j_n}, \mathcal{I}_{zm_{j_n}}$  in magnitudes but opposite in directions. The assignment of the effective spin parameters  $s_n, \sigma_n$  above is in direct conformity with the role of the Standard Model neutron spin with respect to the experimental determination of neutron magnetic moment based on magnetic resonance method [1f].

#### 4. Electron–proton electromagnetic interaction

We shall below derive for the electron  $e$  and proton  $p$  comprising the model neutron their interaction force  $\mathbf{F}$ , the corresponding potential  $V$  and stationary-state Hamiltonian  $H$  based on first principles laws of electromagnetism and (the solutions of Sec 2 of) relativistic kinematics and quantum-mechanics. We shall continue to work in the CM frame, i.e. in terms of the unsuperscripted mass and space-time variables which will directly enter the electromagnetic interactions below, and for simplicity the time  $t$  instead of  $t_e, t_p$ ; the partial time  $t_e, t_p$  effect will be included afterward by a projecting factor ( $f_t^2$ ). In this section,  $\mathbf{r}$  or  $\mathbf{r}_{ij}$  refers to the  $e, p$  separation distance starting at  $\mathbf{r}_p$ , ending at  $\mathbf{r}_e$ , as in Figs 1a, c; its magnitude is equal to that of  $\mathbf{r}$  or  $\mathbf{r}_{ij}$  of Sec 2.4, Fig 1b.

Consider the  $e, p$  system in a precessional-orbital state  $j = l - l_{TP}$ ,  $m_j = -j$ , with the  $e, p$  spins  $S_{pz}, S_{ez}$  in the  $+z$  direction, i.e. antiparallel with  $J_{z-j}$  (as in Figs 1a,b or Fig 2a for  $j = 1 - \frac{1}{2} = \frac{1}{2}$ ,  $m_j = -\frac{1}{2}$ ). Firstly, the proton of a charge  $+e$  produces at the electron at  $\mathbf{r}_{ij}$  apart a (transformed) Coulomb field  $\mathbf{E}_p(r_l) = (e/4\pi\epsilon_0 r_l^2) \hat{\mathbf{r}}_{ij}$  (in SI units here and below);  $\hat{\mathbf{r}}_{ij} = \mathbf{r}_{ij}/r_l$  is a unit vector pointing from  $p$  to  $e$ .  $|\mathbf{E}_p|$  is amplified from its rest-frame value  $E_p^0$  by a factor  $\propto (1/r^2)/(1/(r^0)^2) = \gamma^2 = 1/f_c$  and hence has a narrowed profile at a point  $\mathbf{r}$  perpendicular to its motion  $\phi$  direction by an inverse factor,  $f_c$ . And so are the magnetic fields below. Furthermore, the proton is in relative precessional–orbital motion in clockwise sense at the tangential velocity  $\mathbf{v}_p$  about the CM in the  $x'y'$  plane, and in spin motion at the tangential velocity  $\mathbf{v}_{p_{xy}}^s$  in the  $x_p^s y_p^s$  plane (Sec 3.1). The latter, after a projection on to the  $x'y'$  and hence  $x''y''$  plane, may be effectively represented (Eq A.3, Appendix A) as two point half-charges located at  $-\bar{a}, \bar{a}$  from  $\mathbf{r}_p$  on the  $x''$  axis and moving oppositely at velocities  $-\bar{v}_p^{s''}, +\bar{v}_p^{s''}$  in  $-y'', +y''$  directions. So  $p$  produces at  $e$  magnetic fields  $\mathbf{B}_p^{orb} (= -\mathbf{v}_p \times \mathbf{E}_p/c^2)$  and  $\mathbf{B}_p^s(r_l \pm \bar{a}) (= \pm |\bar{v}_p^{s''} \times \mathbf{E}_p(r_l \pm \bar{a})|/c^2)$  along the  $z'$  direction given as (the transformed Biot-Savart law),

$$\begin{aligned} \mathbf{B}_p^{orb}(r_l) &= \frac{e\mathbf{v}_p \times \mathbf{r}_{ij}}{4\pi\epsilon_0 c^2 r_l^3} = -\frac{e\mathbf{r}_{ij} \times (\frac{m_e m_p}{M})\mathbf{v}_j}{4\pi\epsilon_0 m_p c^2 r_l^3} = -\frac{\sqrt{4l^2 - 1} e\hbar \hat{z}'}{8\pi\epsilon_0 m_p c^2 r_l^3}; \quad \mathbf{B}_p^s(r_l \pm \bar{a}) = \frac{\pm \frac{1}{2} e\bar{\mathbf{v}}_p^{s''} \times (\mathbf{r}_{ij}/r_l)}{4\pi\epsilon_0 c^2 (r_l \pm \bar{a})^2}, \\ \mathbf{B}_p^s(r_l) &= \mathbf{B}_p^s(r_l - \bar{a}) + \mathbf{B}_p^s(r_l + \bar{a}) = \frac{-e\bar{a}\bar{\mathbf{v}}_p^{s''} \times (\mathbf{r}_{ij}/r_l)}{2\pi\epsilon_0 c^2 r_l^3 (1 - \frac{\bar{a}^2}{r_l^2})^2} = \frac{-\eta^2 g_p e\hbar \cos\theta_j \hat{z}'}{4\pi\epsilon_0 m_p c^2 r_l^3 C_{1l}}, \quad C_{1l} = \left(1 - \frac{\bar{a}^2}{r_l^2}\right)^2 \end{aligned} \quad (29)$$

The last of Eqs (29a) is given after substituting (3b) for  $\mathbf{v}_p$  and (16.1)' for  $\mathbf{r}_{ij} \times (\frac{m_e m_p}{M})\mathbf{v}_j$ . The last of Eqs (29c) is given after substituting (A.1a), (A.3b) for  $\bar{a}, \bar{v}_p^{s''}, a$  for  $a_p$ , and (19) for  $av_p^s m_p \cos\theta_p^s/g_p (= \frac{1}{2}\hbar)$ . The negative signs in the two final results indicate  $\mathbf{B}_p^{orb}, \mathbf{B}_p^s$  to be in the  $-z'$  direction each.

In the  $\mathbf{E}_p$  and  $\mathbf{B}_p^{orb} + \mathbf{B}_p^s = \mathbf{B}_p$  fields of the proton (cf Fig 1a), the electron at  $\mathbf{r}_{ij}$  apart, with an effective charge  $q_e = -f_c e$ , and in precessional–orbital and spin motions at the tangential velocities  $\mathbf{v}_e$  (about the CM) and  $\bar{v}_e^{s''}$  in the  $x'y'$  plane, in clockwise and counter-clockwise senses, is acted by an electromagnetic force along the  $\mathbf{r}_{ij}$  direction according to the Lorentz force law,

$$\mathbf{F}_{pe}(r_l, \theta_j) = -f_c e \mathbf{E}_p(r_l) + f_t^2 [\mathbf{F}_{pe,m}^{orb-orb}(r_l, \theta_j, t) + \mathbf{F}_{pe,m}^{s-orb}(r_l, \theta_j, t) + \mathbf{F}_{pe,m}^{s-s}(r_l, \theta_j, t)], \quad (30)$$

$$\text{where } \mathbf{F}_{pe,m}^{orb-orb} = -e\mathbf{v}_e \times \mathbf{B}_p^{orb} = -\frac{e\mathbf{r}_{ij} \times (\frac{m_e m_p}{M})\mathbf{v}_j}{m_e r_l} B_p^{orb} = -\frac{(4l^2 - 1)e^2 \hbar^2 \hat{r}_{ij}}{16\pi\epsilon_0 m_e m_p c^2 r_l^4}, \quad (31)$$

$$\mathbf{F}_{pe,m}^{s-orb} = -e\mathbf{v}_e \times \mathbf{B}_p^s = -\frac{e\mathbf{r}_{ij} \times (\frac{m_e m_p}{M})\mathbf{v}_j}{m_e r_l} |\mathbf{B}_p^s| = \frac{(2l - 1)\eta^2 g_p e^2 \hbar^2 \hat{r}_{ij}}{8\pi\epsilon_0 m_e m_p c^2 r_l^4 C_{1l}}, \quad (32)$$

$$\mathbf{F}_{pe,m}^{s-s} = -\frac{\partial V_{pe,m}^{s-s}}{\partial r_l} \hat{r}_{ij} = |\boldsymbol{\mu}_{ez}^s \cos\theta_j| \frac{\partial |\mathbf{B}_p^s|}{\partial r_l} \hat{r}_{ij} = -\frac{3\eta^2 g_e g_p e^2 \hbar^2 \cos^2\theta_j \hat{r}_{ij}}{16\pi\epsilon_0 m_e m_p c^2 r_l^4 C_{1l}}. \quad (33)$$

$f_c$  is the fraction of the  $e$ -charge sphere momentarily facing the narrowed  $\mathbf{E}_p$  profile at  $\mathbf{r}_{lj}$ . Eq (3a) for  $\mathbf{v}_e$  and again (16.1)' for  $r_l(\frac{m_e m_p}{M})v_j$  are used in (31),(32). In (33),  $V_{pe,m}^{s-s} = -|\boldsymbol{\mu}_{ez}^s||\mathbf{B}_p^s| \cos\theta_j$  is the magnetic potential of the spin-spin interaction;  $\boldsymbol{\mu}_{ez}^s$  is an intensive quantity at  $\mathbf{r}_e$ , hence not affected by the  $B_p$  profile narrowing, and is given by Eq (20a).  $\mathbf{F}_{m0}^{s-s} = -\int_0^{2\pi} e\mathbf{v}_e^s \times \mathbf{B}_{pz}^s(r_l)d\phi_e^s = 0$ ;  $\frac{\partial|\mathbf{B}_p^s|}{\partial r_l} = -\frac{3B_p^s}{r_l}$ .  $f_t^2$  projects the product term  $v_e v_p$  contained in each component magnetic force to  $v'_e v'_p$  which actually enters the interaction;  $\mathbf{F}_{pe}(r_l, \theta_j) \equiv \mathbf{F}_{pe}(r_l, \theta_j, t_e, t_p)$  is implicitly meant.  $v'_e v'_p = (v_e M/m_p)(v_p M/m_e) = f_t^2 v_e v_p$  (Sec 2.1), so  $f_t^2 = M/\mathcal{M}$ . A repulsion  $\mathbf{F}_{pe}^{rep} = A_{rep}\hat{r}/r_l^{N+1}$  at short range, relative to the magnetic interaction strength at the distance  $r \sim 10^{-18}$  m, may generally also present but is omitted for the intermediate range of interest here. Given the presumed  $S_{ez}, S_{pz}, J_{z-j} = \frac{1}{2}, \frac{1}{2}, -j$  configuration in units  $\hbar$  here, all the three component magnetic forces (for  $l > 0$  for  $F_{pe,m}^{orb-orb}, F_{pe,m}^{s-orb}$ ) acted by  $p$  on  $e$  above are optimally in the  $-\mathbf{r}_{lj}$  direction and hence attractive.  $\mathbf{F}_{pe}$  is therefore in the  $-\mathbf{r}_{lj}$  direction and maximally attractive. Any alteration of the relative orientations between  $S_{ez}, S_{pz}, J_{z-j}$  will render some or all of the component magnetic forces repulsive. An alteration of  $S_{ez}, S_{pz}, J_{z-j}$  as a whole, i.e. from the configuration (i) to (ii) of Eqs (21) or from Fig 2a to 2b, retains all component magnetic forces attractive, and hence a total force  $\mathbf{F}_{pe}$  the same as given in (31), or  $F_j$  given in (34) below.

Similarly,  $e$  produces at  $p$  at  $-\mathbf{r}_{lj}$  apart the electromagnetic fields  $\mathbf{E}_e$  and  $\mathbf{B}_e$ , and forces given as  $f_c e \mathbf{E}_e$ ,  $f_t^2 \mathbf{F}_{ep,m}^{orb-orb} = -f_t^2 \mathbf{F}_{pe,m}^{orb-orb}$ ,  $f_t^2 \mathbf{F}_{ep,m}^{s-orb} = -f_t^2 \mathbf{F}_{pe,m}^{s-orb} \frac{g_e}{g_p}$ ,  $f_t^2 \mathbf{F}_{ep,m}^{s-s} = -f_t^2 \mathbf{F}_{pe,m}^{s-s}$ . The action and reaction forces for the  $e, p$  in equilibrium must be equal in magnitude and opposite in direction (Newton's third law); the magnitude may be here represented by the geometric mean as  $F = \sqrt{|\mathbf{F}_{pe}||\mathbf{F}_{ep}|} = \sum_{\lambda, \lambda'} \sqrt{|\mathbf{F}_{pe}^\lambda||\mathbf{F}_{ep}^{\lambda'}|} \delta_{\lambda\lambda'}$ , where  $\lambda, \lambda'$  indicate the different component forces. The last equation needs to hold for the action and reaction to maintain detailed balance upon any small variation of the independent variables such as  $\mathbf{r}_{lj}$ . The final total (attractive) force of  $p$  on  $e$  in equilibrium in the  $j = l - l_{TP}, m_j = -j$  state is therefore, suffixing  $j$  after  $\mathbf{F}$  explicitly,  $\mathbf{F}_j(r_l, \theta_j) = -[f_c e \sqrt{|\mathbf{E}_p||\mathbf{E}_e}| + f_t^2 \sum_{\lambda} \sqrt{|\mathbf{F}_{pe,m}^\lambda||\mathbf{F}_{ep,m}^\lambda|}] \hat{r} = -f_c e \mathbf{E}_p + f_t^2 [\mathbf{F}_{pe,m}^{orb-orb} + \mathbf{F}_{pe,m}^{s-orb} \frac{\sqrt{g_e g_p}}{g_p} + \mathbf{F}_{pe,m}^{s-s}]$ . Substituting Eqs (31)–(33) into the foregoing we obtain this force in explicit and scalar form,

$$F_j(r_l, \theta_j) = -\frac{e^2}{4\pi\epsilon_0 r_l^2} (f_c + f_m) \simeq -\frac{e^2 f_m}{4\pi\epsilon_0 r_l^2} = -\frac{f_t^2 e^2 \hbar^2 C_{0j}}{16\pi\epsilon_0 m_e m_p c^2 r_l^4}, \quad (34)$$

$$f_m = \frac{f_t^2 \hbar^2 C_{0j}}{4m_e m_p c^2 r_l^2}, \quad C_{0j} = (4l^2 - 1) + \frac{(2l-1)\sqrt{g_e g_p}}{2C_{1l}} + \frac{3g_e g_p \eta^2 \cos^2 \theta_j}{C_{1l}}. \quad (35)$$

The negative sign indicates that  $F_j$  is attractive. The approximation in Eqs (34) is given for  $f_m \gg f_c = 1/\gamma^2$ . For  $j = \frac{1}{2}$  ( $l = 1$ ), using the solution values from Sec 6 gives  $f_m = \hbar^2 c^2 C_{0\frac{1}{2}}/m_e m_p c^4 r_{1m}^2 \simeq 6.9$  which indeed is  $\gg f_c = 1/\gamma^2 \simeq 5.7 \times 10^{-11}$ .

$j = 0$  yields  $J_0 = 0$ ,  $B_p^{orb} = 0$ , and hence zero orbit-orbit and orbit-spin interactions. The resultant system, even if possible to also form a bound state by the finite spin-spin interaction only, is not a viable candidate of the neutron, at least because it does not contain a confined antineutrino. For  $j \geq \frac{1}{2}$ , the three component magnetic forces are each finite and attractive.  $j = \frac{1}{2}$  therefore is the lowest possible (eigen) state of the  $e, p$  bound by an attractive magnetic force at the separation scale  $\sim 10^{-18}$  m (Sec 6), has a confined antineutrino, and has the correct spin  $\frac{1}{2}$  (Sec 3). The  $j = \frac{1}{2}$  state is therefore a liable candidate for (the ground state of) the neutron. For  $j = \frac{1}{2}$  ( $l = 1$ ), hence  $\cos\theta_{\frac{1}{2}} = 1/\sqrt{3}$ , and  $m_e = km_p = 1.3165m_p$  (Sec 3), hence  $f_t^2 = \frac{(m_e + m_p)^2}{m_e m_p} = \frac{(k+1)^2}{k} \simeq 4$ , Eq (34), the corresponding interaction potential  $V_{\frac{1}{2}}$  and Hamiltonian

$H_{\frac{1}{2}}$  are written as, with Eqs (7.2a,b) for  $m_e, m_p$ , and  $T_{\frac{1}{2}}$  given in Sec 2.4,

$$F_{\frac{1}{2}}(r_1, \theta_{\frac{1}{2}}) = -\frac{3A_o C_{0\frac{1}{2}}}{\gamma_e \gamma_p r_1^4}, \quad A_o = \frac{e^2 \hbar^2}{12\pi \epsilon_0 m_e^0 m_p^0 c^2}, \quad C_{0\frac{1}{2}} = 3 + \frac{\sqrt{g_e g_p}}{2C_{11}} + \frac{\eta^2 g_e g_p}{C_{11}}; \quad (36)$$

$$V_{\frac{1}{2}}(r_1, \theta_{\frac{1}{2}}) = -\int_{\infty}^{r_1} F_1(r) dr = \frac{r_1 F_1(r_1)}{3} = -\frac{A_o C_{0\frac{1}{2}}}{\gamma_e \gamma_p r_1^3} = -\frac{e^2 \hbar^2 C_{0\frac{1}{2}}}{12\pi \epsilon_0 m_e m_p c^2 r_1^3} = \frac{e^2 \hbar^2 C_{0\frac{1}{2}}}{48\pi \epsilon_0 \mathcal{M}^2 c^2 r_1^3}; \quad (37)$$

$$T_{\frac{1}{2}} = C_{k\frac{1}{2}} V_{\frac{1}{2}}, \quad C_{k\frac{1}{2}} = \frac{\gamma 9\pi \epsilon_0 M c^2 r_1}{(\gamma + 1) e^2 C_{0\frac{1}{2}}}; \quad H_{\frac{1}{2}}(r_1, \theta_{\frac{1}{2}}) = T_{\frac{1}{2}} + V_{\frac{1}{2}} = V_{\frac{1}{2}}(1 - C_{k\frac{1}{2}}). \quad (38)$$

The last of Eqs (37) is given after substituting the relation  $m_e m_p = \gamma_e \gamma_p m_e^0 m_p^0 = \gamma^2 \mathcal{M}^0 \frac{M^0}{\gamma^\dagger \mathcal{M}^0} \doteq 4 \mathcal{M}^2$ , by use of (8.1b) for  $\gamma_e \gamma_p$ , (8.2e) for  $\gamma_M$ ,  $\gamma^\dagger = 450.960$  given after (10).

### 5. $e, p$ disintegration. $\beta$ decay

Suppose that an afore-described (free) neutron, being in stationary state of the Hamiltonian  $H_{\frac{1}{2}}$  at initial time earlier, is now perturbed by an excitation or external-interaction Hamiltonian  $H_I = H_I^0 + H_I^1 = H_I^1$  given in the CM frame; evidently  $H_I^0 = 0$ . So the bound  $e, p$  are in the final ( $f$ ) state disintegrated into free particles  $e, p$ , with the  $e, p$  at an effective infinite separation  $r_\infty$  such that  $V_{\frac{1}{2}f}(r_\infty) = 0$ . The removal of the central force, say acted by the proton on the electron  $e$  in the  $-\mathbf{r}_{1\frac{1}{2}}$  direction implies a deceleration of  $e$  along that direction, thereby subjecting  $e$  to a deceleration or Bremsstrahlung radiation. Provided no exertion of external torque on the neutron, the angular momentum must be conserved before (being a quantum  $S_{\bar{\nu}_e} = -\frac{1}{2}\hbar$  in  $-z$  direction) and after the deceleration radiation. The electromagnetic radiation emitted is therefore necessarily in the form of a rotational energy flux so as to convey the same angular momentum quantum  $-\frac{1}{2}\hbar$  in the  $z$  direction, and the same rotational kinetic energy  $T_{\bar{\nu}_e} = T_{\frac{1}{2}}$  provided also no exchange of the kinetic energy with the surrounding. The rotational radiation energy flux emitted resembles directly an antineutrino,  $\bar{\nu}_e$ , which is now free. The equation of the foregoing (disintegration) reaction straightforwardly is

$$n \rightarrow p + e + \bar{\nu}_e$$

i.e. this describes a neutron  $\beta$  decay. The final-state total Hamiltonian has the general form  $H_{\frac{1}{2}f} = V_{\frac{1}{2}f}(r_\infty) + T_{\frac{1}{2}f} = 0 + T_{\frac{1}{2}f}$ . The emitted particles would convey a certain translational kinetic energy  $T_{tr}$  as converted from the total mass difference before and after neutron decay. This energy  $T_{tr}$  is of MeV scale (a scale as is also known from  $\beta$  decay experiment) which is  $\ll T_{\frac{1}{2}}$  of GeV scale. Omitting this  $T_{tr}$ , in the case of  $T_{\bar{\nu}_e} = T_{\frac{1}{2}}$ , we have  $T_{\frac{1}{2}f} = T_{\frac{1}{2}} + T_{tr} \simeq T_{\frac{1}{2}}$ , and  $H_{\frac{1}{2}f} = 0 + T_{\frac{1}{2}f} \simeq T_{\frac{1}{2}}$ .

The energy condition for the neutron  $\beta$  decay to occur is  $H_I = H_{\frac{1}{2}f} - H_{\frac{1}{2}}$ . Substituting in it the equation for  $H_{\frac{1}{2}f}$  above and (38c) for  $H_{\frac{1}{2}}$  gives

$$H_I = T_{\frac{1}{2}} - (V_{\frac{1}{2}} + T_{\frac{1}{2}}) = -V_{\frac{1}{2}} = \frac{A_o C_{0\frac{1}{2}}}{\gamma_e \gamma_p r_1^3} \quad \text{or} \quad (39)$$

$$G_F = H_I \left( \frac{4}{3} \pi r_1^3 \right) = \frac{A_o C_{0\frac{1}{2}}}{\gamma_e \gamma_p} = \frac{e^2 \hbar^2 C_{0\frac{1}{2}}}{12\pi \epsilon_0 m_e m_p c^2} = \frac{e^2 \hbar^2 C_{0\frac{1}{2}}}{48\pi \epsilon_0 \mathcal{M}^2 c^2}, \quad C_{0\frac{1}{2}} = \frac{4\pi C_{0\frac{1}{2}}}{3}, \quad (40)$$

where  $(\frac{4}{3}\pi r_1^3)$  is the volume in which the electron is confined about the proton. By virtue of its physical significance, the product term  $G_F = H_I (\frac{4}{3}\pi r_1^3)$  in (40b) is directly identifiable with the CM-frame counterpart of the Fermi (coupling) constant  $G_F^{\text{lab}}$ .

$G_F^{\text{lab}}$  is experimentally determined (as  $G_F^{\text{exp}}$ ) from the neutron lifetime, denoted by  $\tau^{\text{lab}}$  here as is usually measured in the lab frame, on the basis of the quantum theoretical relation  $G_F^{\text{lab}} \propto 1/\sqrt{\tau^{\text{lab}}}$ . The neutron under consideration may be generally in motion, say at a velocity  $u_{\text{cm}}^{\text{lab}}$  in a fixed  $X$  direction. The (model) neutron mass in this direction is (cf Sec 2.3)  $m_n^{\text{lab}} \doteq M^{\text{lab}} = \gamma_{\text{cm}}^{\text{lab}} \langle M \rangle = \gamma_{\text{cm}}^{\text{lab}} M^0$ , where  $\gamma_{\text{cm}}^{\text{lab}} = (1 - (u_{\text{cm}}^{\text{lab}})^2/c^2)^{-1/2}$ . Its component masses are formally  $m_e^{\text{lab}} = (\gamma_{\text{cm}}^{\text{lab}})^{\kappa} m_e$ ,  $m_p^{\text{lab}} = (\gamma_{\text{cm}}^{\text{lab}})^{\kappa} m_p$ , i.e. each in effect augmented by a factor  $(\gamma_{\text{cm}}^{\text{lab}})^{\kappa}$ , where  $\kappa$  is a certain (positive) exponent resulting from the mapping of  $u_{\text{cm}}^{\text{lab}}$  onto the instantaneous interaction direction of  $e, p$ . So Eqs (40a), here re-written from its original form as  $G_F = \frac{e^2 \hbar^2 C_{0\frac{1}{2}}}{12\pi\epsilon_0 m_e m_p c^2} = \frac{A_1}{m_e m_p}$ ,  $A_1 = \frac{e^2 \hbar^2 C_{0\frac{1}{2}}}{12\pi\epsilon_0 c^2}$ , transformed to the lab frame is formally

$$G_F^{\text{lab}} = \frac{A_1}{m_e^{\text{lab}} m_p^{\text{lab}}} = \frac{A_1}{(\gamma_{\text{cm}}^{\text{lab}})^{2\kappa} m_e m_p} = \frac{G_F}{(\gamma_{\text{cm}}^{\text{lab}})^{2\kappa}} \propto \frac{1}{(\gamma_{\text{cm}}^{\text{lab}})^{2\kappa} \sqrt{\tau^0}} = \frac{1}{\sqrt{\tau^{\text{lab}}}} \quad (41)$$

where  $\tau^0$  denotes the lifetime of a neutron at rest. (41) suggests that for a fast moving neutron such that  $u_{\text{cm}}^{\text{lab}2}/c^2 > 0$  and  $\gamma_{\text{cm}}^{\text{lab}} > 1$  appreciably each, the neutron life time  $\tau^{\text{lab}} = (\gamma_{\text{cm}}^{\text{lab}})^{2\kappa} \tau^0$  will appear appreciably "dilated", as the result of a reduced internal (magnetic) interaction strength, or reduced Fermi constant. For a neutron at rest of major concern in this paper,  $G_F$  identifies with  $G_F^{\text{lab}}$  as measured for a rest or slow-moving neutron. We shall continue to speak of  $G_F$ .

Multiplying  $\frac{137 \times 12 \mathcal{M}^2 c^2}{\hbar^3 c C_{0\frac{1}{2}}}$  on both sides, rearranging, the last of Eqs (40a) is written as

$$\frac{G_F (137 \times 12 \mathcal{M}^2 / C_{0\frac{1}{2}}) c^2}{\hbar^3 c} = \frac{137 e^2}{4\pi\epsilon_0 \hbar c}; \quad \text{or} \quad (42)$$

$$\frac{G_F M_{\text{ef}}^2 c^2}{\hbar^3 c} = \frac{g_{\text{neu}}^2}{\hbar c}, \quad M_{\text{ef}} = \left( \frac{137 \times 12 \mathcal{M}^2}{C_{0\frac{1}{2}}} \right)^{1/2} = \frac{40.546 \mathcal{M}}{\sqrt{C_{0\frac{1}{2}}}} \doteq \frac{23.042 m_p}{\sqrt{C_{0\frac{1}{2}}}}, \quad g_{\text{neu}}^2 = \frac{137 e^2}{4\pi\epsilon_0}; \quad (43)$$

or  $G_F = \frac{g_{\text{neu}}^2 (\hbar c)^2}{M_{\text{ef}}^2 c^4}$ .  $M_{\text{ef}}$  is an effective mass; for the last of Eqs (43b)  $m_e = 1.3165 m_p$  is used;  $\frac{e^2}{4\pi\epsilon_0 \hbar c} = \frac{g_H^2}{\hbar c} = \frac{1}{137} = \alpha_H (= \frac{v_{1H}}{c})$  corresponds to the fine structure constant of the hydrogen atom (and  $v_{1H}$  the orbiting velocity of electron relative to proton thereof). Placing the  $\alpha_H$  value in the right side of (42) yields unity,  $\frac{137 \times e^2}{4\pi\epsilon_0 \hbar c} = 1$ . In analogy, the fine structure constant for the model neutron is by definition  $\alpha_{\text{neu}} = v_{\frac{1}{2}}/c$ , and thus  $\alpha_{\text{neu}} \doteq 1$  for  $v_{\frac{1}{2}} \doteq c$  given in Sec 6. Based on its unity value, and on the physical significance of the dynamical variables, say  $\frac{g_{\text{neu}}^2}{\hbar c}$  on its right side compared to  $\frac{g_H^2}{\hbar c}$ , Eq (43a) is immediately identifiable as the equation for  $\alpha_{\text{neu}}$ ,

$$\alpha_{\text{neu}} = \frac{v_{\frac{1}{2}}}{c} \equiv 137 \alpha_H (\doteq 1) = \frac{g_{\text{neu}}^2}{\hbar c} = \frac{G_F M_{\text{ef}}^2 c^2}{\hbar^3 c} \quad (44)$$

In the GWS theory,  $G_F$  is given the formula  $G_F^{\text{GWS}} = \frac{g_w^2 \sqrt{2} (\hbar c)^2}{M_w^2 c^4}$ , where  $g_w^2 = \frac{e^2}{8\epsilon_0 \sin^2 \theta_w}$ . Equating  $G_F^{\text{GWS}}$  with  $G_F$  of (40a) gives a first-principles microscopic expression for  $M_w$ , accordingly  $M_z$ ,

$$M_w = \left( \frac{3\sqrt{2} \pi m_e m_p}{2C_{0\frac{1}{2}} \sin^2 \theta_w} \right)^{1/2} = \left( \frac{3\sqrt{2} \pi}{2C_{0\frac{1}{2}} \sin^2 \theta_w} \right)^{1/2} m_p; \quad M_z = M_w / \cos \theta_w \quad (45)$$

It is well appreciated in the literature that, whilst the  $G_F$  value is absolutely determined by the lifetime of the neutron in question, the  $M_w$  value (as  $M_{\text{ef}}$  in Eq 44) is dependent on the definition or choice of the coupling constant  $g_w^2$  (as  $g_{\text{neu}}^2$  in Eq 44);  $g_{\text{neu}}^2$  in (44) is uniquely specified for



$v_{\frac{1}{2}}$  is separately known. In terms of the  $e, p$ -neutron model,  $M_w$ , or  $M_{ef}$ , represents essentially the (reduced) mass of the  $e, p$  particles in the binding and hence resistive potential field  $V_{\frac{1}{2}}$ .  $V_{\frac{1}{2}}$  resembles the Higgs field. The  $M_w$ , or  $M_{ef}$ , of a neutron is highly relativistically augmented (Sec 6) over that of a hydrogen, primarily as the result of the relative velocity of  $e, p$  within a neutron being so high as to approach  $c$ . Moreover, the  $e, p$  interaction in a neutron is predominately magnetic, and in a hydrogen electrostatic.

## 6. Numerical evaluation

Equations (36)–(40) are specified effectively by four independent variables  $\bar{a}$ ,  $r_1$ ,  $v_{\frac{1}{2}}$ , and  $\gamma(v_{\frac{1}{2}}, c)(= \gamma_e \gamma_p / \gamma_M)$  ( $\gamma_M$  is given if  $\gamma$  is given), to be determined each. We need four independent constraints for quantitatively determining these and subsequently the remaining dynamical variables. Equation (1d) would ordinarily serve as one basic constraint: it describes a stable state condition under which the central force  $\mathbf{F}$  on mass  $\mathcal{M}$  counterbalances with the inertial (or here centrifugal) force  $\mathcal{M} \frac{d^2 \mathbf{r}}{dt^2}$ . It may be checked (App Appendix B) that at a  $r_1$  value satisfying Eq (1d), the lifetime of the  $e, p$  system however is not an optimum. This suggests that the neutron candidate  $e, p$  system, if opted for a maximum lifetime, is not in stable state. We shall choose the maximum lifetime condition here on the basis that a real free neutron indeed is "meta" stable only, with a relatively short lifetime 12 m.

In overall view of the basic solutions from preceding sections, the discussion just made above, and the available key experimental data such as to realistically identify the neutron, we employ (i) the quantisation condition (17a) for  $J_{\frac{1}{2}}^1$ , (ii) a maximum neutron lifetime, hence a minimum  $G_F$ , and (iii) the experimental value of the Fermi constant,  $G_F^{exp}$ , as three basic constraints. These are (re-) written as, on dividing (17a) by  $r_1 \mathcal{M}^0 v_{\frac{1}{2}}$  for (i), and denoting by  $r_{1m}$  the extremal value of  $r_1$  at which  $G_F$  is a minimum,

$$(i) : \quad \gamma = \gamma_M \gamma^\dagger = \frac{\sqrt{3}(\hbar c)c}{2\mathcal{M}^0 c^2 r_1 v_{\frac{1}{2}}} = \frac{D_o c}{r_1 v_{\frac{1}{2}}}, \quad D_o = \frac{\sqrt{3}\hbar c}{2\mathcal{M}^0 c^2} \quad (46)$$

$$(ii) : \quad G_F(r_{1m}) = G_{F.min} \quad (47)$$

$$(iii) : \quad G_F(r_{1m}) = G_F^{exp} = 1.43585(37) \times 10^{-62} \text{ Jm}^3 \quad (\text{data from [1e]}) \quad (48)$$

Since (46a) suggests that  $\gamma \gg 1$  for any  $v_{\frac{1}{2}}$  value not too far below  $c$ , and  $c = c^{lab}$  by the standard assumption, so  $v_{\frac{1}{2}} = c\sqrt{\gamma^2 - 1}/\gamma \simeq c = c^{lab}$ , which serves as the fourth constraint here. With this  $v_{\frac{1}{2}}$  value in (46a), we obtain (49a,b) below; further with (8.1b) for  $\gamma_e \gamma_p (= \gamma_M \gamma = \gamma_M^2 \gamma^\dagger)$  and the resultant  $\gamma_M$  from (49b) in (40a), with  $\gamma^\dagger = 450.960$  given in Sec 2.2 (for  $m_e = 1.3165m_p$ ), we obtain (50) below,

$$\gamma = \frac{D_o}{r_1}, \quad \gamma_M = \frac{\gamma}{\gamma^\dagger} = \frac{D_o}{\gamma^\dagger r_1}, \quad (49)$$

$$G_F = \frac{A_o C_{0\frac{1}{2}}}{\gamma_M^2 \gamma^\dagger} = \frac{\gamma^\dagger A_o C_{0\frac{1}{2}} r_1^2}{D_o^2} = \frac{450.960 A_o C_{0\frac{1}{2}} r_1^2}{D_o^2}. \quad (50)$$

$D_o (= 3.3462 \times 10^{-13} \text{ m})$  and  $A_o (= 6.2455 \times 10^{-57} \text{ Jm}^3)$  are constants. provided use the experimental  $g$  values of  $e, p$ ,  $g_e = 2$ ,  $g_p = 5.5857$ , and  $\eta = 1/\sqrt{2}$  (Appendix A). For evaluating  $C_{0\frac{1}{2}}$  (Eqs 40c, 36c), we shall use the experimental  $g$  values of  $e, p$ ,  $g_e = 2$ ,  $g_p = 5.5857$ , and  $\eta = 1/\sqrt{2}$  (Appendix A).  $G_F$  of (50) is then solely dependent on  $r_1, \bar{a}$ . Characteristically,

<sup>1</sup> The eigen value solution (17a) represents directly a Heisenberg relation for  $J_{\frac{1}{2}}$  and the angular interval  $2\pi$ , or alternatively  $2T_{\frac{1}{2}} = C_{k\frac{1}{2}} H_{\frac{1}{2}} / (C_{k\frac{1}{2}} - 1)$  and  $\Delta t_{\frac{1}{2}}$ . The excitation Hamiltonian  $H_I$  is not necessarily conjugated with the  $\Delta t_{\frac{1}{2}}$ , but generally with some other time interval subjecting to a Heisenberg relation depending on the excitation scheme.

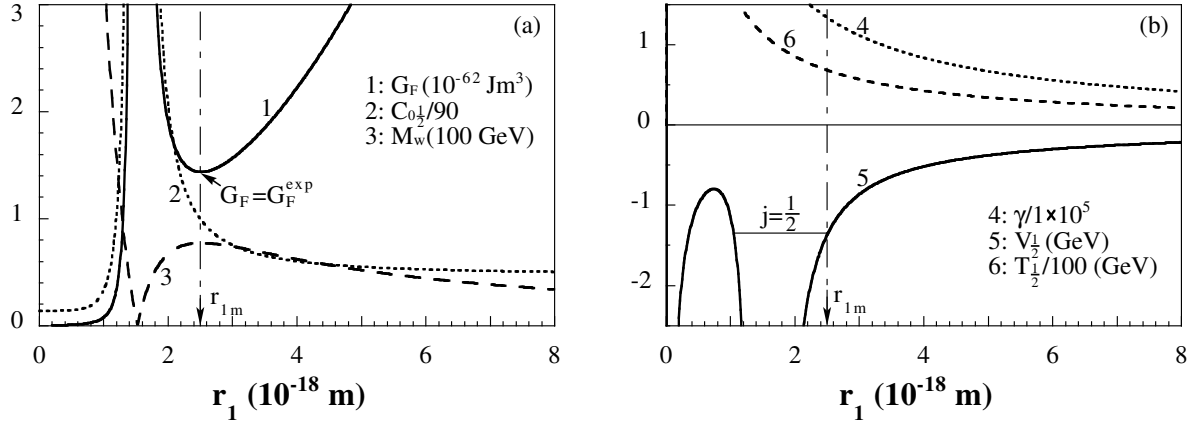


**Figure 3.** (a)  $G_F = H_I r_1^3$ ,  $C_{0\frac{1}{2}}$ ,  $M_w$  (curves 1,2,3), and (b)  $\gamma$ ,  $V_{\frac{1}{2}} = -H_I$ ,  $T_{\frac{1}{2}}$  (curves 4,5,6) as functions of  $r_1$  computed from Eqs (50), (36c), (45), (49a), (37), (38a) for  $\bar{a} = 1.5391(8) \times 10^{-18}$  m. At  $r_1 = r_{1m} = 2.5369(5) \times 10^{-18}$  m,  $G_F = G_F^{exp} = 1.43585(37) \times 10^{-62}$  Jm<sup>3</sup>.

for a specified  $\bar{a}$  value, the  $G_F(r_1)$  vs  $r_1$  function presents an extremal point at a (uniquely specified)  $r_1$ ,  $r_{1m}$ , at which  $G_F(r_{1m})$  is a minimum (Eq 47), as in Fig 3a, although this is not generally equal to  $G_F^{exp}$ .  $G_F(r_{1m})$  increases monotonically with  $\bar{a}$ . Computing  $G_F(r_{1m})$  as a function of  $\bar{a}$  over a range of  $\bar{a}$  values, a unique  $\bar{a}$  is found at  $\bar{a} = 1.5391(8) \times 10^{-18}$  m at which  $G_F(r_{1m}) = G_F^{exp}$  (Eq 48),  $r_{1m} = 2.5369(5) \times 10^{-18}$  m,  $\gamma = 1.3190 \times 10^5$  (Eq 49a), and  $C_{0\frac{1}{2}} = (\frac{4\pi}{3}) \times 3(1 + 1.3952 + 4.6633) = 88.69$  (Eqs 40b, 36c). Note that the  $\bar{a}$  value obtained is in accordance with the order of magnitude of the neutron charge radius,  $\sim 1.4 \times 10^{-18}$  m, measured by electron-neutron scattering experiment (see also Sec 2.3).

With the  $\bar{a}$ ,  $r_{1m}$  (hence  $C_{0\frac{1}{2}}$ ),  $v_{\frac{1}{2}}$ ,  $\gamma$  values obtained, all the remaining dynamical variables and functions may be evaluated. For the fixed  $\bar{a} = 1.5392 \times 10^{-18}$  m value, the  $G_F$ ,  $C_{0\frac{1}{2}}$ ,  $M_w$  (using the average experimental value  $\sin^2 \theta_w = 0.23$ ),  $\gamma$ ,  $V_{\frac{1}{2}} (= -H_{\frac{1}{2}})$ , and  $T_{\frac{1}{2}}$  vs.  $r_1$  functions, computed from Eqs (50), (36c), (45a), (46a), (37), (38a) are as shown in Figs 3a,b (curves 1-6).  $r_1 = r_{1,\min}$  lies as expected in the region where  $-\partial V_{\frac{1}{2}}(r)/\partial r = F_{\frac{1}{2}}(r) < 0$ , and  $V_{\frac{1}{2}}(r) < 0$ . At  $r_1 = r_{1m}$ ,  $V_{\frac{1}{2}} = -H_I = -1.310$  GeV,  $T_{\frac{1}{2}} (\simeq \mathcal{M}c^2) = 67.36$  GeV,  $H_{\frac{1}{2}} (\simeq E_{tot,\frac{1}{2}}) = 66.05$  GeV,  $M_w = 77.23$  GeV. Furthermore specifically, with the  $\gamma$  value in (49b),(9a),(b), we obtain  $\gamma_M = 292.483$ ,  $\gamma_e = \gamma_M \frac{(M^0 + \Gamma)}{2m_e^0} = 3.0537(6) \times 10^5$ , and  $\gamma_p = \gamma_M \frac{(M^0 - \Gamma)}{2m_p^0} = 126.33$ , which are  $\gg 1$  each. So the particles  $e, p$  within the neutron are travelling at velocities  $v'_e, v'_p \simeq c$  measured in their local space and time coordinates  $\mathbf{r}_e, t_e, \mathbf{r}_p, t_p$  (Eqs 5) in the (non-inertial) CM frame; and so is the total mass  $M$  at the CM relative to  $e, p$ . The total kinetic energy of  $e, p$  in these absolute terms is given by substituting the  $v'_e, v'_p, m_e (= km_p), m_p$  values in (12.2) as  $T'_e + T'_p \doteq (k+1)m_p c^2 = 2.3165\gamma_p m_p^0 c^2 = 2.3165 \times 118.53 = 2 \times 137.29$  GeV. Substituting  $m_e = km_p$  into Eqs (3a,b) gives the  $e, p$  velocities measured in time  $t$ ,  $v_e = \frac{m_p}{M} v = \frac{c}{k+1} = 0.43c$ ,  $v_p = -\frac{m_e}{M} v = -\frac{kc}{k+1} = -0.57c$ ; and in turn the above values into Eq (11.2) gives the corresponding total kinetic energy  $T_e + T_p = km_p (\frac{c}{k+1})^2 + m_p (\frac{kc}{k+1})^2 = \frac{k}{k+1} m_p c^2 = 0.56831 \times 118.53 = 67.36$  GeV, equal to the solution value for  $T_{\frac{1}{2}} = \mathcal{M}c^2$  earlier. The non-inertial frame motion contributes an amount  $(T'_e + T'_p) - (T_e + T_p) = (k+1)m_p c^2 - \frac{k}{k+1} m_p c^2 = \frac{k^2+k+1}{k+1} m_p c^2 = 1.75m_p c^2$ . The exceedingly large kinetic energy apparently is mainly consumed to contract the size of the system.

The author expresses thanks to emeritus scientist P-I Johansson for his private financial and moral support of the author's research, to Kissemiss Johansson for his joyful companion when the unification researches were carried out, and to Professor C Burdick for providing the opportunity of presenting this wok at the ISQS23 conference, Tech Univ, Prague, at which the

author also very much enjoyed interesting discussions with a number of participants.

### Appendix A. Mapping of the spin current loop on to reduced geometries

Consider here the circular spin current loop of proton as projected in the  $x_p^s y_p^s$  plane, spinning at tangential velocity  $v_{pxy}^s$  about the  $z_p^s$  axis passing through  $\mathbf{r}_p$  in spin up state as in Sec 3.1.  $dq_p = \rho_{pxy} a_p d\phi_p^s$  is a charge element at  $\boldsymbol{\xi}_p(\phi_p^s)$  on it. The magnetic field produced by this spin current loop at a distance  $\mathbf{r}$  from  $\mathbf{r}_p$  has the general form (Biot-Savart law)  $\mathbf{B}_p^s(\mathbf{r}) = \int d\mathbf{B}_{p\theta}^s(\mathbf{r}') = \int \frac{dq_p \mathbf{v}_{pxy}^s \times \mathbf{r}'}{4\pi\epsilon_0 c^2 r'^3}$ , where  $\mathbf{r}' = \mathbf{r} + \boldsymbol{\xi}_p(\phi_p^s)$ . The integration in algebraic terms is a complex problem. We below reduce the current loop to simpler geometries to facilitate an effective algebraic expression for the field (Eq 29b, Sec 4).

Consider first this field produced at a point at distance  $x_p^s = |\mathbf{r}|$  from  $\mathbf{r}_p$  on the positive  $x_p^s$  axis,  $\mathbf{B}_p^s(x_p^s = |\mathbf{r}|)$ . The problem has the obvious symmetry that the left-half current loop produces at  $x_p^s$  a magnetic field  $\mathbf{B}_{pL}^s (\propto \mathbf{v}_{pxy}^s \times \mathbf{x}_p^s) > 0$  in  $+z$  direction, and the right-half a field  $\mathbf{B}_{pR}^s < 0$  in  $-z$  direction. The total field  $\mathbf{B}_{pR}^s - \mathbf{B}_{pL}^s = \mathbf{B}_p^s(x_p^s = |\mathbf{r}|)$  is in  $-z$  direction. Furthermore, on either half loop the differential  $d\mathbf{B}_p^s$  fields produced by all charge elements as associated with the  $y$ -component velocities add up, and with  $x$ -component velocities cancel out. So, in so far as the same  $\mathbf{B}_{pL}^s, \mathbf{B}_{pR}^s$  are in effect produced, the left- and right- half spin current loops may be further reduced to two point half-charges  $+\frac{1}{2}e, +\frac{1}{2}e$  located at effective distances  $-\bar{a}, \bar{a}$  from  $\mathbf{r}_p$  on the  $x_p^s$  axis and moving oppositely at velocities  $-\bar{v}_{pxy}^s, \bar{v}_{pxy}^s$  in the  $-y_p^s, +y_p^s$  directions, where

$$\bar{a} = \eta a, \quad \bar{v}_{pxy}^s = \bar{v}_p^s \cos \theta_p^s, \quad \bar{v}_p^s = \bar{a} \omega_p^s = \eta a \omega_p^s = \eta v_p^s, \quad v_p^s = a \omega_p^s. \quad (A.1)$$

We have set  $a = a_p = a_e = \frac{1}{2}(a_e + a_p)$  here; so  $\bar{a}$ , as  $a$ , is effective also in its representing the average radius of the  $e, p$  charges. In analogy to  $r = r^0/\gamma$ ,  $a$  is contracted<sup>2</sup> from its rest value  $a^0$  according to  $a = a^0/\gamma_a$ .

By virtue of its physical significance,  $\bar{a}$  should be such that the moments of inertia of the right and left point half-charges about the  $z_p^s$  axis,  $I_R^{point}, I_L^{point} (= I_R^{point})$ , are equal to those of the half current loops about  $z_p^s$ ,  $I_R^{loop}, I_L^{loop} (= I_R^{loop})$ . Let  $m_p^*$  be the effective mass uniformly distributed along the full current and in turn on the full charge, and hence a mass  $\frac{1}{2}m_p^*$  on each half loop and in turn at each half point charge. The moments of inertia of one point half charge and one half loop are known as, written for the right ones,

$$I_R^{point} = \frac{1}{2}m_p^* \bar{a}^2, \quad I_R^{loop} = \int_0^\pi x^2 dm_p^* = 2 \int_0^{\pi/2} (a_p \cos \phi)^2 \frac{(m_p^*/2)}{\pi} d\phi = \frac{m_p^* a^2}{4} \quad (A.2)$$

The equality  $I_R^{loop} = I_R^{point}$  gives  $\frac{1}{2}\bar{a}^2 (= \frac{1}{2}(\eta a)^2) = \frac{1}{4}a^2$ , so  $\eta = 1/\sqrt{2}$ . Accordingly, the spin angular momentum of the right point half-charge is  $S_{pR} = I_R^{point} \omega_p^s (= I_R^{loop} \omega_p^s) = \frac{1}{2}m_p^* \bar{a}^2 \omega_p^s = \frac{1}{2}m_p^* \bar{a} \bar{v}_p^s$ , and the  $z$  component is  $S_{pRz} = S_{pR} \cos \theta_p^s = \frac{1}{2}m_p^* \bar{a} \bar{v}_{pxy}^s$ .

Now with respect to a point at a distance  $\mathbf{x}_p^{s''}$  from  $\mathbf{r}_p$  on the  $x''$  axis (Sec 2.4) lying in a plane whose normal is along the  $z'$  or  $z''$  direction and at angle  $\theta_j$  to the  $z$  axis, with  $|\mathbf{x}_p^{s''}| = |\mathbf{x}_p^s| = |\mathbf{r}|$ , the spin angular momentum of the right point half-charge perpendicular to  $x''$  is the projection of  $S_{pRz}$  onto the  $z''$  or  $z'$  direction,

$$S_{pRz}'' = S_{pRz} \cos \theta_j = \frac{1}{2}m_p^* \bar{a} \bar{v}_{pxy}^s \cos \theta_j = \frac{1}{2}m_p^* \bar{a} \bar{v}_p^{s''}, \quad \bar{v}_p^{s''} = \bar{v}_{pxy}^s \cos \theta_j = \bar{v}_p^s \cos \theta_p^s \cos \theta_j \quad (A.3)$$

<sup>2</sup> Contractions in charge radius and in the wavelength of matter wave may be comprehended on a common physical ground as follows. Charges and matter waves are distributed energy entities in space each. Two charges or two matter waves by this nature will inevitably repel with one another when attempting to occupy same space. Higher velocities are to facilitate two charges or two matter waves to counterbalance such repulsion to a larger extent, manifesting consequently as the contraction.

## Appendix B. Stable-state solution for $r_l$

Substituting  $\frac{d^2 \mathbf{r}_{lj}}{dt^2} = -\frac{v_j^2}{r_l} \hat{r}_{lj}$ ,  $v_j$  from (16.1)', and  $\mathbf{F}_j$  from (34) into (1d) gives  $-\mathcal{M} \frac{(4l^2-1)\hbar^2 \hat{r}}{4\mathcal{M}^2 r_l^3} = -\frac{f_t^2 e^2 \hbar^2 C_{0j} \hat{r}}{16\pi\epsilon_0 m_e m_p c^2 r_l^4}$ . Cancelling common factors on both sides, sorting, with  $f_t^2 = 4$  for  $m_e = 1.3165m_p$  (Sec 4) and  $M = \gamma_M^{(j)} M^0$  for  $j$ th state, we obtain

$$r_l = \frac{e^2 C_{0j}}{(4l^2 - 1)\pi\epsilon_0 \gamma_M^{(j)} M^0 c^2}. \quad \text{For } j = \frac{1}{2}, l = 1: \quad r_1 = \frac{e^2 C_{0\frac{1}{2}}}{3\pi\epsilon_0 \gamma_M^{(\frac{1}{2})} M^0 c^2}; \quad (B.1)$$

for  $j = \frac{3}{2}$ ,  $l = 2$ ,  $r_2 = \frac{e^2 C_{0\frac{3}{2}}}{15\pi\epsilon_0 \gamma_M^{(\frac{3}{2})} M^0 c^2}$ ,  $C_{0\frac{3}{2}} = 15 + \frac{3\sqrt{g_e g_p}}{2C_{12}} + \frac{9g_e g_p}{10C_{12}}$  given after Eq (35b). For the  $j = \frac{1}{2}$  state, with (36b) for  $C_{0\frac{1}{2}}$ , (29d) for  $C_{11}$ , and  $\bar{a} = 1.53918 \times 10^{-18}$  m, the right side of (B.1b) may be computed as a function of  $r_1$ . Two numerical solutions are found at  $r_1 = 1.440 \times 10^{-18}$ ,  $1.661(7) \times 10^{-18}$  m, at which the two sides of (B.1b) are equal.

- [1] (a) Perkins DH 1982 *Introduction to High Energy Physics*, 2nd ed (Reading: Addison-Wesley); (b) Griffiths D 1987 *Introduction to elementary particles* (New York: Harper & Row); (c) Williams WSC 1992 *Nuclear and Particle Physics* (Oxford: Clarendon); (d) Enge HA 1969 *Introduction to Nuclear Physics* (Massachusetts: Addison-Wesley); (e) Beringer J, et al (Particle Data Group) 2012 *Phys. Rev.* **D86** 010001; (f) Alvarez L and Bloch H 1940 *Phys Rev* **57** 111; Staub HH and Roger EH 1950 *Hel Phys Acta* **23** 63-92.
- [2] (a) Higgs P 1964 *Phys. Lett.* **12** 132; 1964 *Phys. Rev. Lett.* **13** 508-9; *ibid* 321; Englert P and Brout R 1964 *Phys. Rev. Lett.* **13** 321; Gutranik GS, Hagen CR and Kibble TWB 1964 *Phys. Rev. Lett.* **13** 585; (b) Weinberg S 1967 *Phys. Rev. Lett.* **19** 1264; Salam A 1968 in *Elementary particle physics: relativistic groups and analicity, Nobel Symp.* **8**, Svartholm N ed (Stockholm: Almquist & Wiksells) p 367; (c) Glashow SL, Lliopoulos L and Maiani I 1970 *Phys. Rev.* **D2** 1285; (d) 'T Hooft G 1971 *Nucl. Phys.* **B33** 173-99; 1971 *Phys. Lett.* **B37** 195; (e) Fermi E 1934 *Zeit. f. Physik* **88**171; tr Wilson FL 1968 *Am. J. Phys.* **36** 1150-60.